Groundwater Flow and Hydrology in Vicinity of L31N Canal (Miami-Dade, Florida) during 2005-2011

James T. Brock
Brian Fitzgerald
Richard B. Susfalk

June 2012

Prepared by:

Desert Research Institute,
Nevada System of Higher Education

Prepared for:

South Florida Water Management District
West Palm Beach, Florida

Cover Photo:

Aerial oblique view of L31N Canal looking north with Everglades National Park on the west (left), and the L31NS monitoring station on the margin of the marsh, located to the west (left) of the levee access road. Photo: P. Lynch (SFWMD)

Suggested Citation:

Brock, J.T., B. Fitzgerald, and R.B. Susfalk. 2014. Data summary report groundwater flow and hydrology in vicinity of L31N Canal (Miami-Dade, Florida) during 2005-2011. Desert Research Institute, Reno, Nevada. Prepared for South Florida Water Management District. Purchase Order # 4500064939, West Palm Beach Florida.

Revised:

5 September 2014

L31N_2012_Data_Report_5Sep2013_fin.pdf

ACKNOWLEDGEMENTS

Environmental monitoring studies of this magnitude involve contributions and cooperation of numerous agencies and individuals. The data compilation and analysis for this report was partially funded under Purchase Order 4500064939 to Desert Research Institute. Data collection was supported under Contract CPO40310 and Purchase Order 4500016426 from the South Florida Water Management District (SFWMD) to Rapid Creek Research, Inc. Steve Krupa, John Shaffer and Bob Verrastro were the Project Managers at the SFWMD. Cynthia Gefvert compiled background information on the L31N wells. Cindy Bevier assisted with obtaining the historical data from SFWMD's DBHYDRO. The SFWMD supplied materials and equipment for use in the calibration including well screen, gravel pack, calibration tank, metering pumps, and laboratory analysis of the sediment. This project would not have been possible without the guidance and assistance of Kerfoot Technologies, especially Bill Kerfoot and Lina Yang. Jack Donahue advised on electronics design. Thanks are extended to Dan Wermers for his expertise in design and testing of the electronics interface circuitry. Craig Day and Terry Johnson provided fabrication services for the monitoring instruments and automated calibration system. Roinda Plesner provided vital technical assistance during development of the calibration procedure at Rapid Creek Research. David Hibbs of Barr Engineering Co (Ann Arbor, MI) assisted with review of vector analysis used to determine probe direction and magnitude of flow. Lisa Wable and Sophie Baker of Desert Research Institute (DRI) prepared the illustrations. Debi Noack and Maria Vasquez improved the report format. Alan Priddy assisted tirelessly during installation of the field instruments. Niki Swanson contributed to probe calibration and data analysis. We thank Steve Krupa, Bob Verrastro, Cynthia Gefvert, Anne Dodd, and Christopher McVoy for comments that improved earlier drafts of the report.

THIS PAGE INTENTIONALLY LEFT BLANK

CONTENTS

LIST OF FIGURES

LIST OF TABLES

THIS PAGE INTENTIONALLY LEFT BLANK

INTRODUCTION

The purpose of the L-31N Seepage Management Pilot Project (SMPP) was to investigate technologies that can be used to control seepage from Everglades National Park (ENP), while minimizing impacts to Miami-Dade County's West Well field. The SMPP is situated in an area of particularly high transmissivity within the Biscayne Aquifer, where it is desirable to control eastward seepage of groundwater, towards the urban area of Miami-Dade County and to improve water deliveries to the Northeast Shark River Slough within Everglades National Park. As the first step in this project, it was important to understand the current seepage, including direction and rate of flow prior to implementation of seepage control measures. Two groundwater monitoring stations were constructed in 2004 by the South Florida Water Management District (SFWMD) on the eastern border of Everglades National Park. The stations are located on the western levee of the L-31N canal (Figures 1-3).

Each station features four monitor wells to facilitate the measuring of water levels and seepage flow. The four-well clusters at each station are located adjacent to a USGS gaging station in the L31N canal along with a stilling well in the Everglades marsh. The L31NN station is located one mile south of US Highway 41 (Tamiami Trail), and L31NS is located three miles to the south of Tamiami Trail adjacent to a limestone mine and aggregate processing facility. This report summarizes the data collected at the L31NN and L31NS stations during the period 2004-2011. Elevation data from nearby surface and groundwater monitoring wells are included to help provide context for the L31NN and L31NS data.

METHODS

The two well clusters were installed to determine if the seepage was similar at each location. The screened intervals of the monitoring wells at L31NN (Figure 4) and L31NS (Figure 5) were selected to correspond to zones of preferential flow (Cunningham et al. 2006; Table 1). SFWMD also installed at each L31N station a float and shaft encoder within a stilling well to measure the surface water in Everglades National Park (Figure 6). The vertical locations of the sensors in the wells are presented in Table 2. The water levels and temperature data collected in the wells were transmitted to the SFWMD, verified, and stored in the DBHydro database. The flowmeter data were transmitted to Rapid Creek Research (Boise, Idaho), which maintained the instruments and remotely monitored its performance. The data from the L31N gaging stations were collected and then stored in the NWIS (National Water Information System), maintained by U.S. Geological Survey. Water level data are reported to 0.01 ft resolution. All elevations are referenced to NGVD 1929.

Hydrogeologic data collected during drilling and subsequent geophysical logging by Kevin Cunningham and Mike Wacker indicated extremely high hydraulic conductivities (113 ft/s) and macro-porosities within the aquifer (Cunningham et al. 2009).

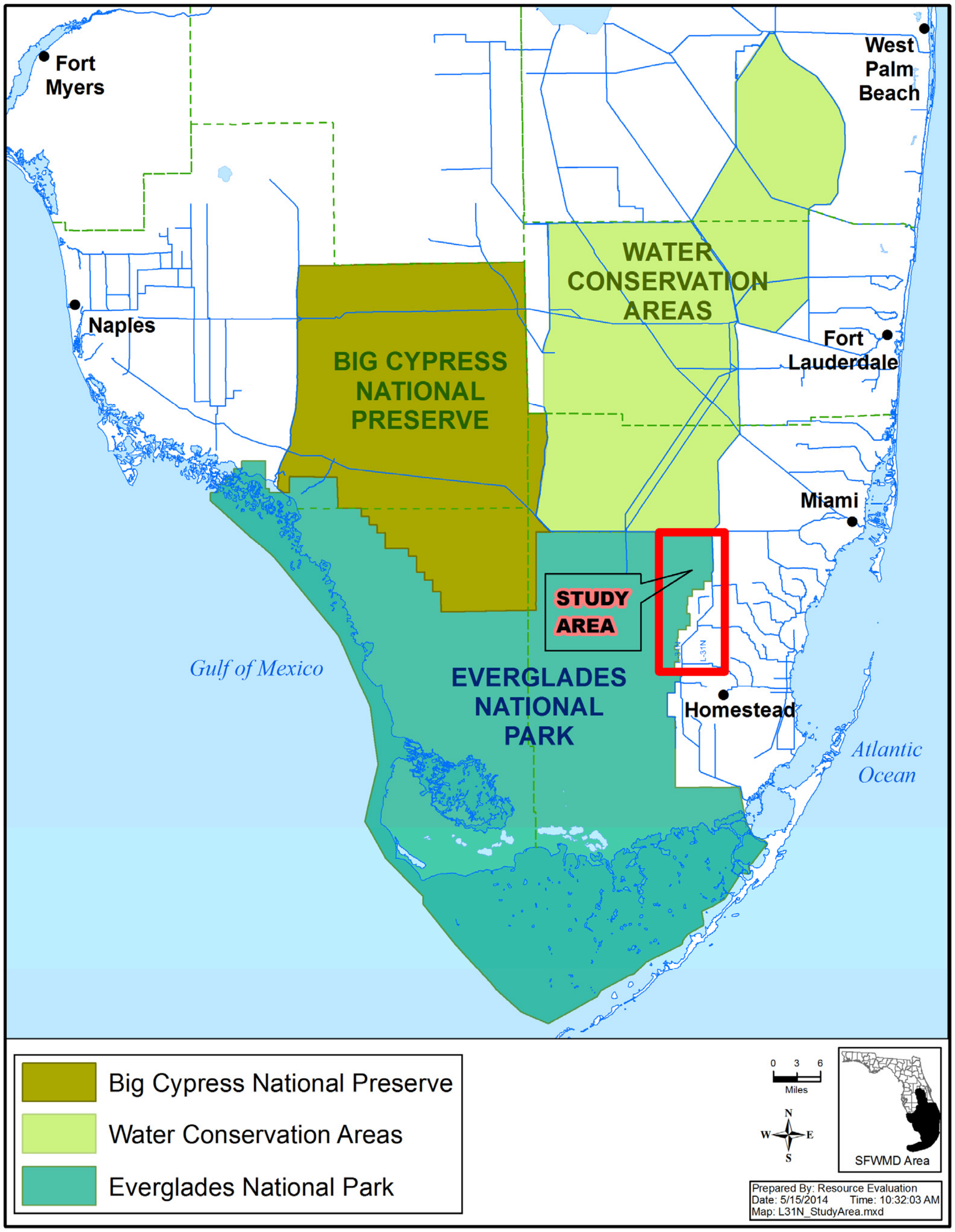

Figure 1. Location of study area in south Florida is indicated by the red rectangle. See Figure 2 for further detail (Source: SFWMD).

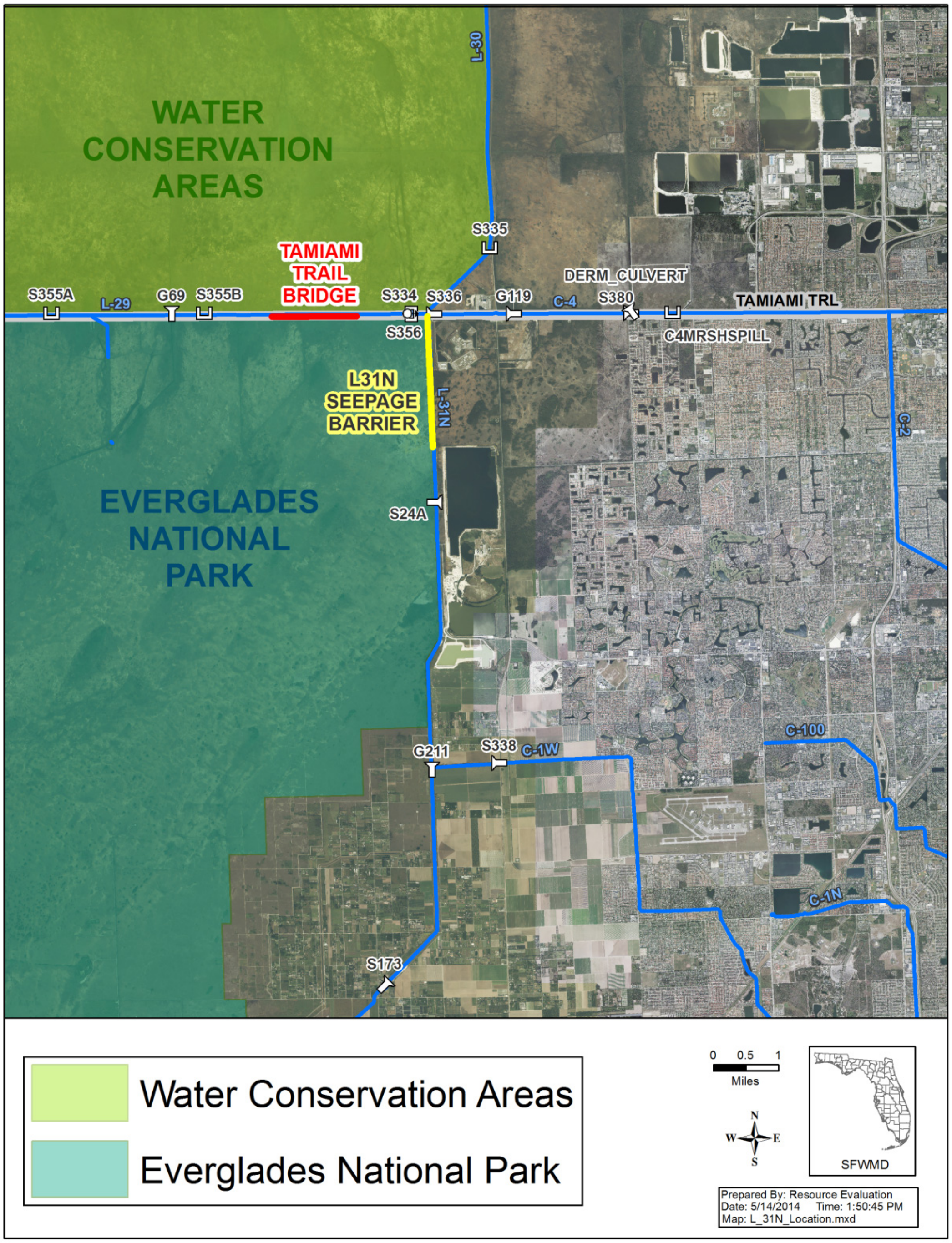

Figure 2. Location map of L-31N area showing roads and water management structures.

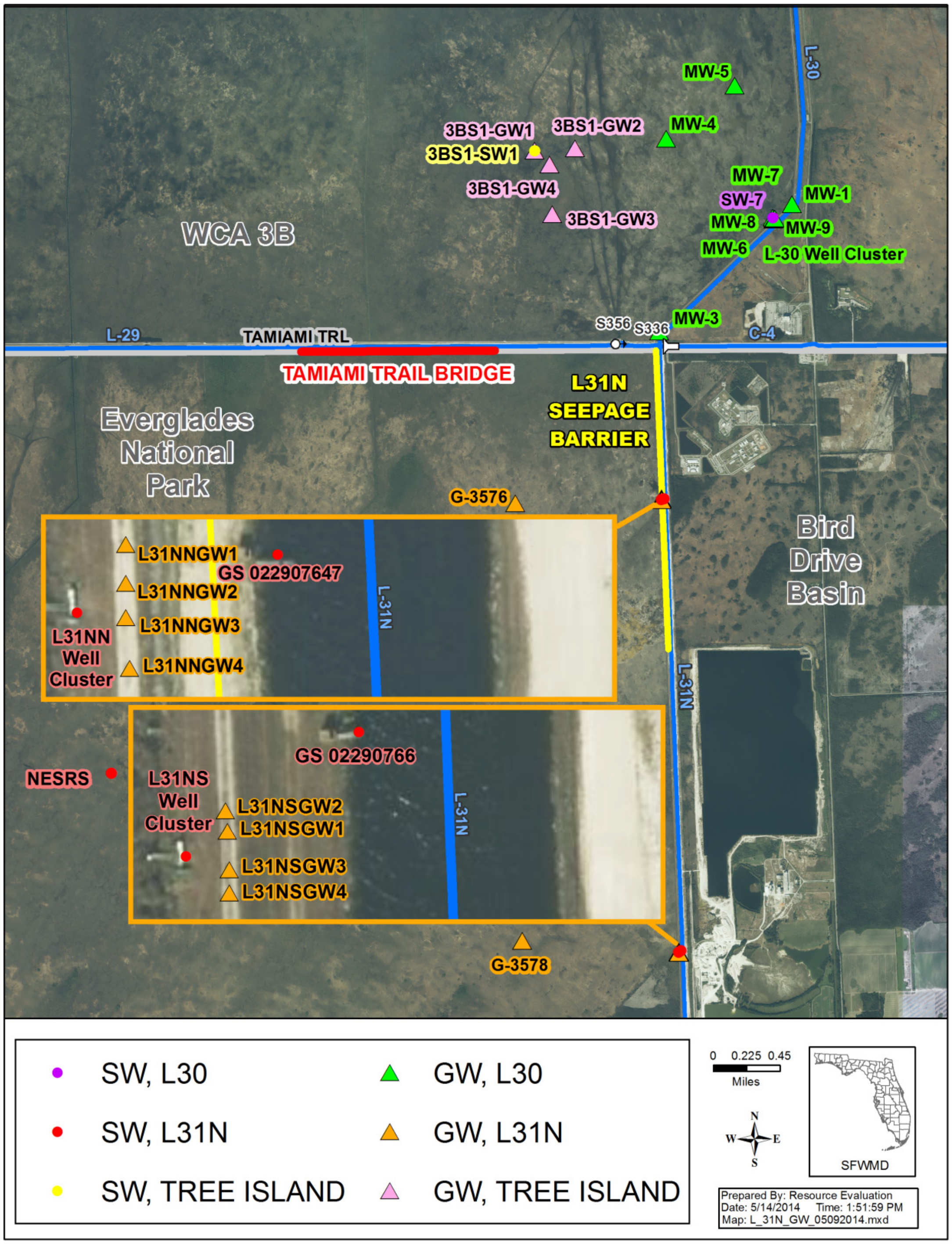

Figure 3. Location Map of monitoring stations in WCA 3B and Northeast Corner of Everglades National Park with inserts detailing L31NN and L31NS well clusters, Miami-Dade, Florida

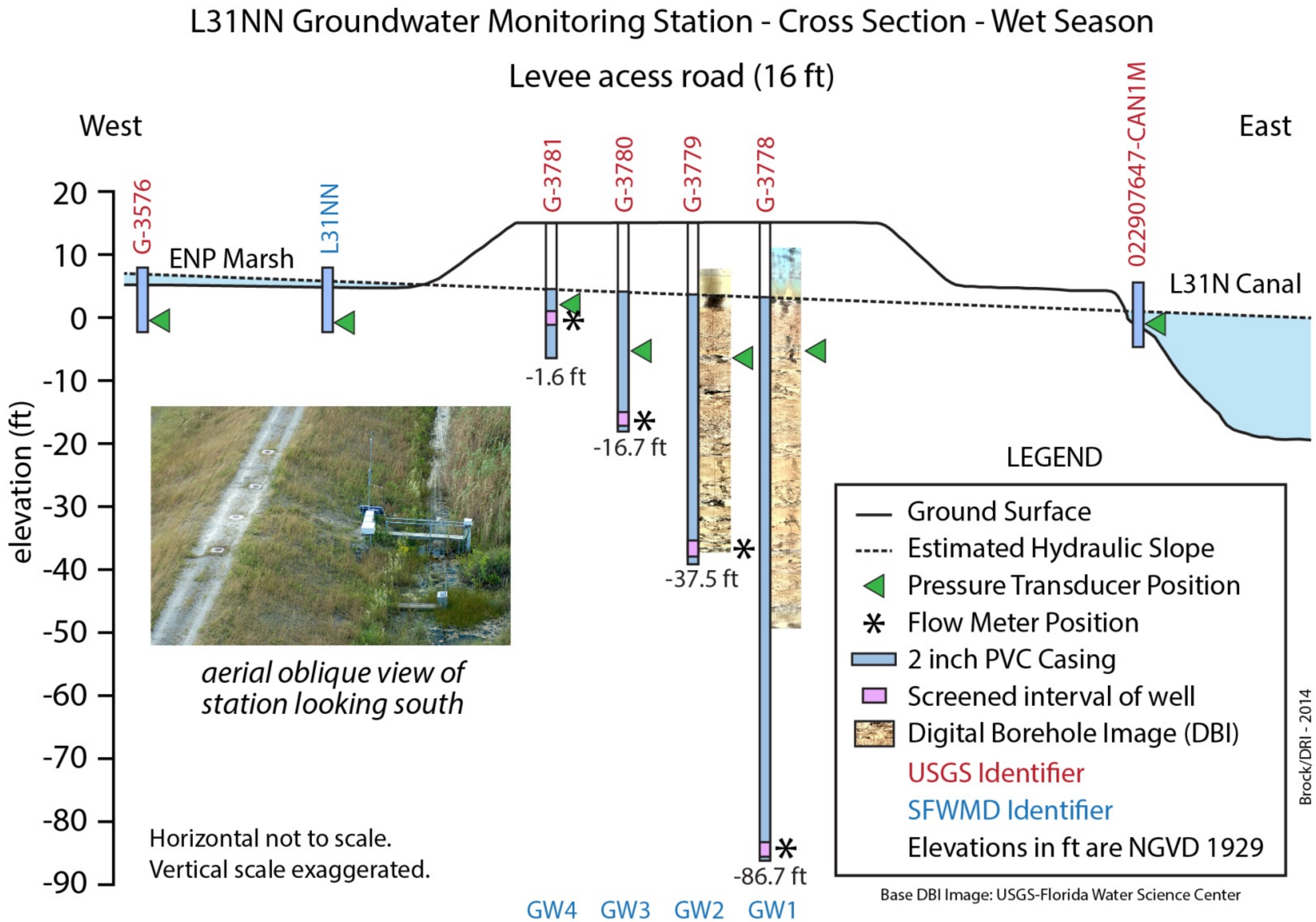

Figure 4. Cross section of L31NN Groundwater Monitoring Station including well G3576 and CAN1 in L31N Canal. Wells are actually aligned north-south on levee access road, but are shown along east-west section for clarity. Elevations given for wells are the center of the screened interval.

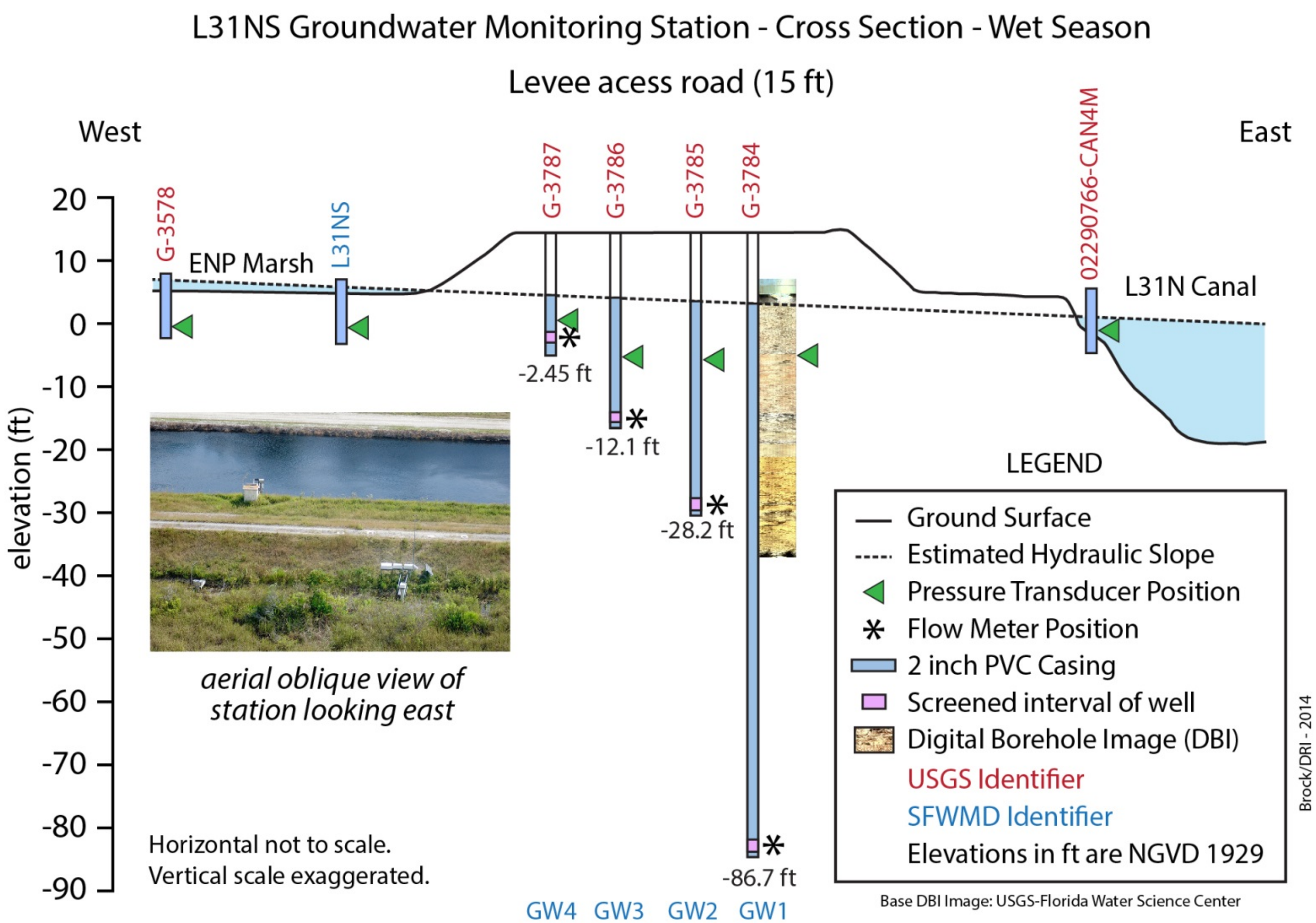

Figure 5. Cross section of L31NS Groundwater Monitoring Station including well G3578 and CAN3 in L31N Canal . Wells are actually aligned north-south on levee access road, but are shown along east-west section for clarity. Elevations given for wells are the center of the screened interval.

Table 1. Well construction data for L31NN and L31NS (Miami-Dade County, Florida).

Station Name	USGS ID	Latitude	Longitude	Ground Surface Elevation	Total Depth of Well	Depth at Bottom of Screen	Screen Length	Screen Slot Size	Well Casing Material SCH40 PVC	Sand (2) Pack at Screen Interval	Elev-ation at Top of Well Screen	Elev-ation at Bottom of Well Screen	Meas-uring Point at TOC (1)
		NAD 1983	NAD 1983	ft (1929 NGVD)	ft	ft	ft	inch			ft (1929 NGVD)	ft (1929 NGVD)	ft (1929 NGVD)
L31NN		25.74626	-80.498013	6.0 (4)									
L31NNGW1	G-3778	25.746342	-80.497875	16.36	103.56	103.26	2.0	0.01	2"	6/20	-85.68	-87.68	15.58
L31NNGW2	G-3779	25.746289	-80.497875	16.15	54.45	54.45	2.0	0.06	2"	1/4" by 1/8"	-36.50	-38.50	15.65
L31NNGW3	G-3780	25.74624	-80.497876	16.39	33.67	33.37	2.0	0.06	2"	1/4" by 1/8"	-15.72	-17.72	15.65
L31NNGW4	G-3781	25.746176	-80.49787	16.49	18.85	18.55	2.0	0.06	2"	1/4" by 1/8"	-15.72	-2.61	15.94
L31NS		25.701976	-80.49631	5.9 (4)									15.21
L31NSGW1	G-3784	25.702012	-80.496186	15.72	100.79	100.49	2.0	0.01	2"	6/20	-83.12	-85.12	15.37
L31NSGW2	G-3785	25.702041	-80.496187	15.83	44.70	44.40	2.0	0.06	2"	1/4" by 1/8"	-27.19	-29.19	15.21
L31NSGW3	G-3786	25.701955	-80.496184	15.63	28.67	28.37	2.0	0.06	2"	1/4" by 1/8"	-11.13	-13.13	15.24
L31NSGW4	G-3787	25.701923	-80.496183	15.86	19.22	18.92	2.0	0.06	2"	1/4" by 1/8"	-1.45	-3.45	15.47

Notes: (1) Determined 12 May 2012

(2) filter pack is washed silica sand

(3) TOC= Top of Casing

(4) Marsh elevation of surface water stilling well

Table 2. Probe Elevations at L31NN and L31NS

Station ID	Common Station Name	DBHYDRO DB Key	Latitude NAD 1983	Longitude NAD 1983	Elevation Top of Casing NGVD 1929 Note 1	Elevation Pressure Transducer NGVD 1929 Note 4	Elevation Hanger Pin Flow-meter NGVD 1929	Dist Hang Bottom of Flow-meter Note 2	Dist Hang Center of Flow-meter Note 3	Elevation Center of Flow-meter NGVD 1929	Description
L31NN	L31NN	SO629	25.746260	-80.498013							ENP Marsh Surface
L31NNGW1	G-3778	S5133	25.746342	-80.497875	15.630	-4.36	15.55	102.54	102.44	-86.81	
L31NNGW2	G-3779	S5131	25.746289	-80.497875	15.704	-4.37	15.62	52.98	52.88	-37.18	
L31NNGW3	G-3780	S5129	25.746240	-80.497876	15.679	-5.82	15.60	33.08	32.98	-17.30	
L31NNGW4	G-3781	S5127	25.746176	-80.497870	16.000	2.09	15.92	17.88	17.78	-1.78	
L31NS	L31NS	SO631	25.701976	-80.496310							ENP Marsh Surface
L31NSGW1	G-3784	S5141	25.702012	-80.496186	15.260	-4.00	15.18	99.40	99.30	-84.04	
L31NSGW2	G-3785	S5139	25.702041	-80.496187	15.420	-3.88	15.34	43.91	43.81	-28.39	
L31NSGW3	G-3786	S5137	25.701955	-80.496184	15.280	-3.82	15.20	28.35	28.25	-12.97	
L31NSGW4	G-3787	S5135	25.701923	-80.496183	15.510	2.54	15.43	14.88	14.78	0.73	

Notes:

(1) Keith and Schnars 2006. . L31N Surveyers Report. Project Number 16434.00. Submitted to SFWMD, October 14, 2006.
(2) Measured 14 Feb 2012. J. Brock.
(3) Distance from bottom to center of Fuzzy Packer = 0.1 ft
(4) Determined from Datalogger, Karl Snyder (SFWMD) 15 May 2012

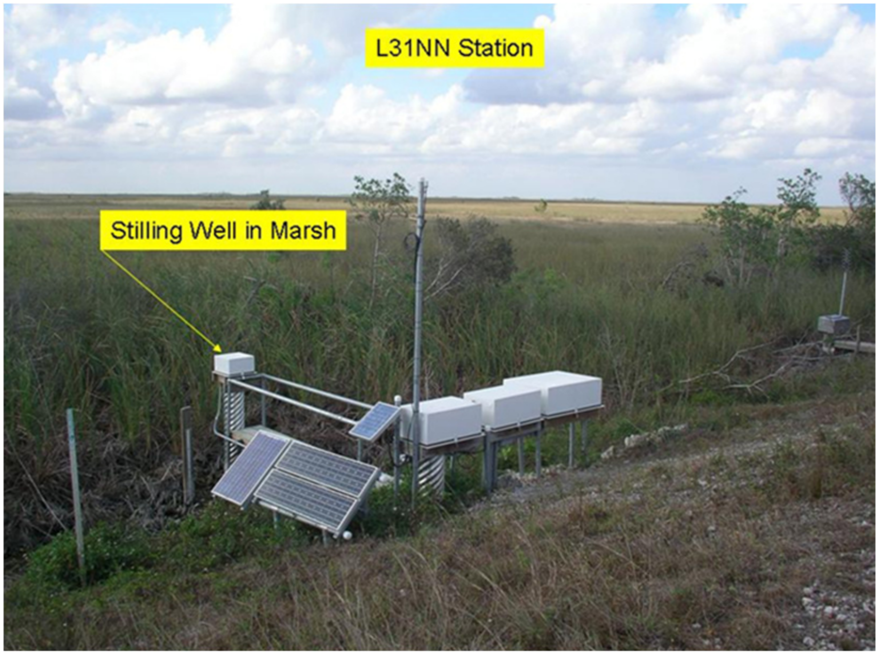

Figure 6. Photograph looking northwest of L31NN Monitoring Station. The appearance of the L31NS Station is similar.

Water Surface Elevation and Temperature

Each monitor well is instrumented with a pressure transducer, to record both water levels and temperature, and a horizontal groundwater flow meter, to measure the velocity and direction of groundwater movement. In this report, the term "groundwater flow" is used to describe regional or sub-regional flow directions, trends and general conditions; whereas "seepage" will refer to water that is moving around or under a barrier, and is tending to be influenced by a vertical feature. The stilling wells contain a float and shaft encoder. Water level data are converted to water surface elevation (WSE) based on regular (approximately bimonthly) site visits when the level data are calibrated against instantaneous manual measurements taken using a chalk and steel tape (SFWMD 2006).

Heat-Pulse Flowmeter

The Cypress Groundwater Flow Meter (GWFM) in use at the L31NN and S groundwater monitoring stations is functionally equivalent to the heat-pulse groundwater flowmeter used by Krupa et al. (2001) in their preliminary assessment of velocity at the Miami-Dade wellfield. The heat-pulse flowmeter uses thermal transmission within a saturated porous media composed of glass beads to provide the basis for groundwater flow measurement. The probe creates a heat pulse that is transmitted through the saturated porous matrix. Net movement of the interstitial water creates a thermal conductance bias, which is proportional to the rate of water flow (Kerfoot 1982).

The glass beads in the probe's porous cap provide more consistent results than direct placement in soil or native porous material (Kerfoot and Massard 1985). Although the beads constitute a differing hydraulic conductivity in the vicinity of the probe, this difference is addressed by calibrating the probe in the porous media that surrounds the well screen. The probes were calibrated in the laboratory using the procedure described in Kerfoot (1982, 1988) and Brock and Krupa (2014). A sediment-filled tank served as the calibration chamber, with water circulated by means of a flow metering pump (See Appendices B and D). The overall goal of the calibration was to create a known flow field in the laboratory that duplicates as closely as possible the conditions that exist with the field installation. The flowmeters were installed and became operational during 2006 and continue to collect data at present (2013).

Flow Measurement and Data Acquisition System

The heater on the flowmeter is pulsed for 30-second duration on a regular basis, typically once every 60 minutes. When energized, the heat is conducted in a radial direction from the heat source. Under conditions of groundwater flow, the heat field tends to move in the direction of flow, thereby causing a heated plume to be conducted through the saturated porous matrix towards the downstream temperature sensor. A Campbell Scientific CR23X datalogger controls the heating cycle and makes measurements of the thermistors once each second.

The heat pulse flow probes were calibrated in the laboratory at Rapid Creek Research, Inc. (Boise, Idaho) using procedures developed by Kerfoot (1998). Calibration was accomplished using an aquifer simulator containing well screen and gravel pack similar to that employed in construction of the L31N wells. Probes were calibrated over a range of 10-180 ft/day (see Appendix B). There was no adjustment made for flow magnification by the well screen and flow probe, therefore velocities are considered “unadjusted.”

RESULTS AND DISCUSSION

Precipitation and Hydroperiod

Ultimately, the goal of understanding and managing seepage under the L31N levee is to be able to improve biological conditions within the portion of the remnant Everglades included in Everglades National Park. As a wetland that has been dried out both by decreased inflows (blockage by Tamiami Trail/U.S. 41) and increased outflows (seepage towards the Miami-Dade water supply wellfield), improved biological conditions will result from increased water depths and increased hydroperiods. Water depths and hydroperiods are in turn direct drivers of seepage. The hydroperiod for the Everglades marsh adjacent to L31N and measured rainfall are presented here for the period of record of the groundwater flow measurements.

Over the 7-year study period, the hydroperiod varied substantially from year to year (Figure 7). Comparison with rainfall at nearby S-336 (Figure 8) suggests that there is no simple relationship between annual rainfall and the hydroperiod at either site.

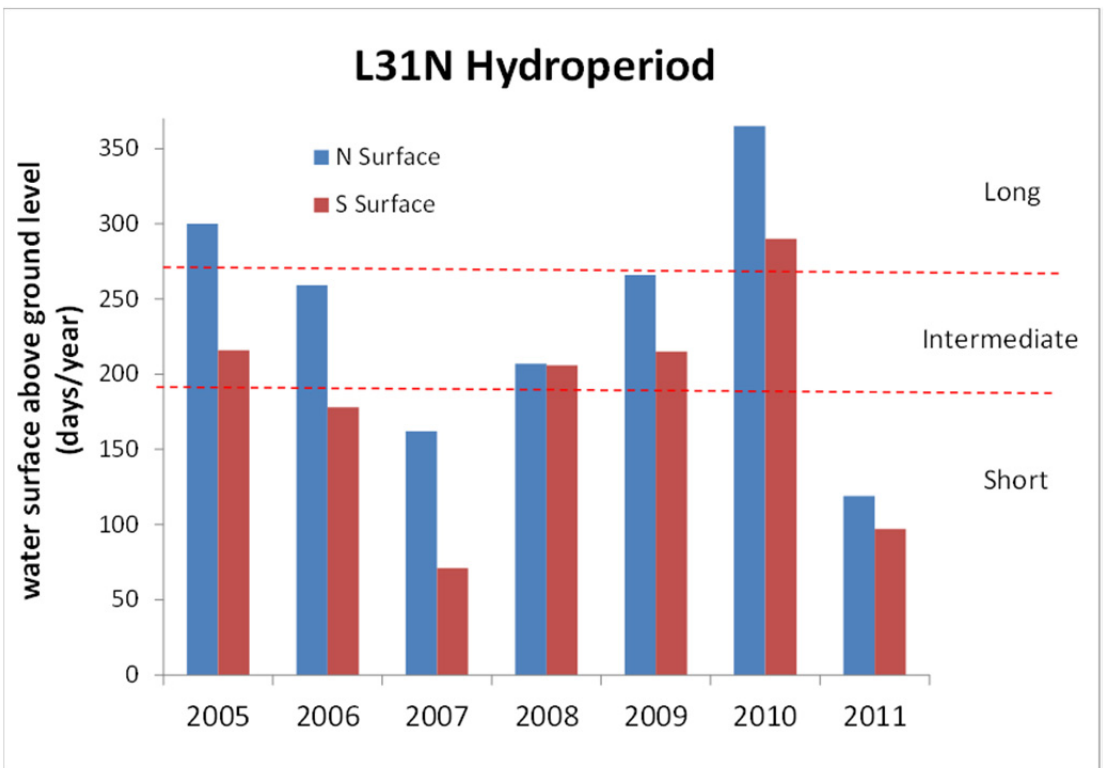

Figure 7. Marsh hydroperiod for the L31NN (N) and L31NS (S) sites during 2005-2011. Short (less than 6 months/year), Intermediate (6-9 months/year), and Long (over 9 months/year) hydroperiod ranges shown for reference (Kushlan 1990).

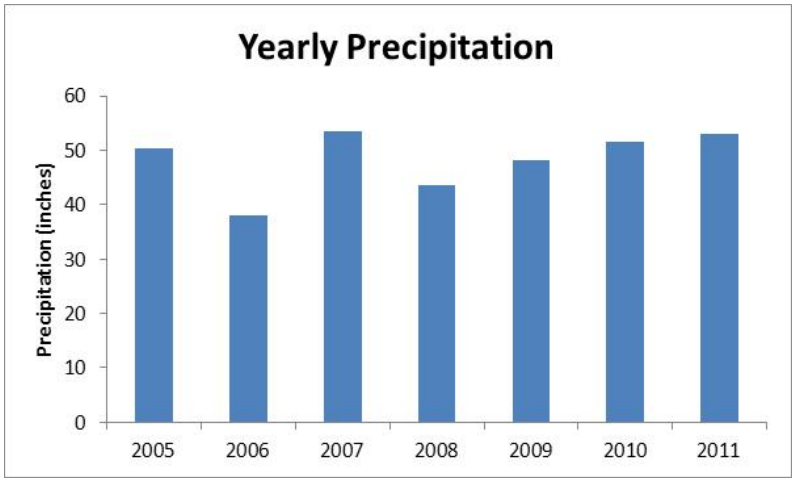

Figure 8. Annual precipitation at S-336, 2005-2011. Note that interannual variation (ca. 20 inches) is large relative to the average total (ca. 47 inches).

Years 2007 and 2011 experienced the highest annual rainfalls, yet had the shortest hydroperiods. While these two years suggest an (illogical) inverse relationship between annual rainfall and hydroperiod, other years suggest the opposite. Factors not evaluated in this study that may influence hydroperiod include possible time lags between rainfall and water depth, and operation of water management structures.

The seasonality of precipitation is illustrated at S336 (Figure 9). In a typical year the dry season occurs December through May and the wet season during the months of June through November.

Water Surface Elevation

Comparison of the water surface elevations (both surface water and groundwater) measured at the north and south sites (Figures 10 and 11) reveal both similarities and important differences. Both sites are within the Northeast Shark Slough portion of Everglades National Park, which originally fell within the peat-based ridge and slough landscape (McVoy et al. 2011). Prior to human water management, i.e., prior to approximately 1900, sloughs within these areas experienced long, occasionally multi-year hydroperiods and surface water depths with long term average annual lows and highs of 1 foot (30 cm) and 3 feet (90 cm), respectively (McVoy et al. 2011). The surface water tables shown in Figures 10 and 11 indicate that both sites are much drier now, with water depths peaking at only 1 to 1.5 feet above the marsh bed rather than 3 feet, and the minimum extending to -2 feet, i.e., below the marsh surface rather than remaining 1 foot or more above the marsh surface. Hydroperiods are correspondingly short now compared to pre-water management.

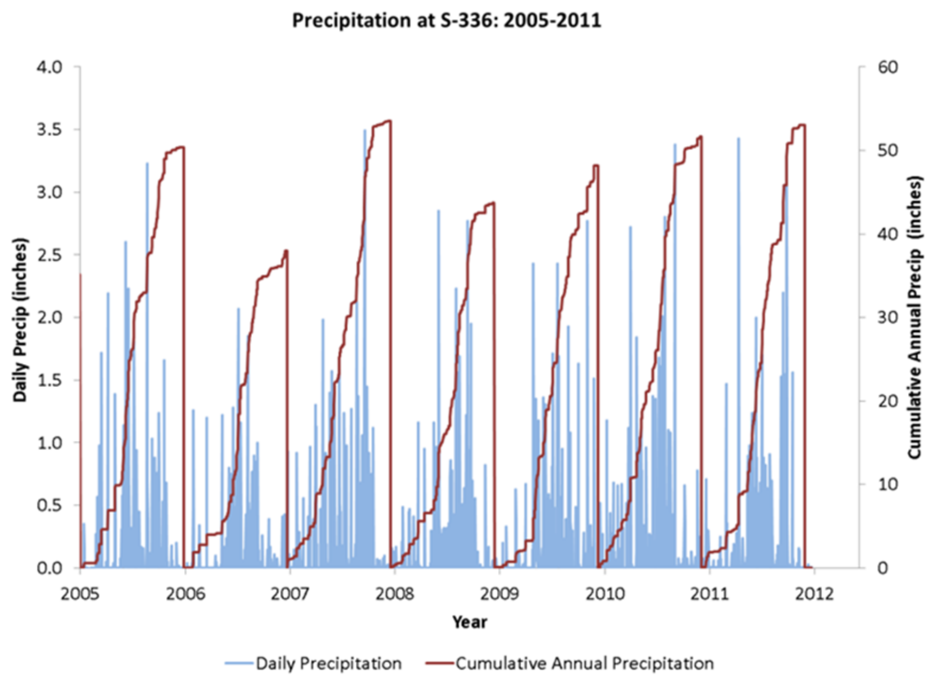

Figure 9. Daily and cumulative precipitation near the L31NNN and L31NNS sites (S-336 structure). Annual precipitation is re-zeroed on December 31 of each year.

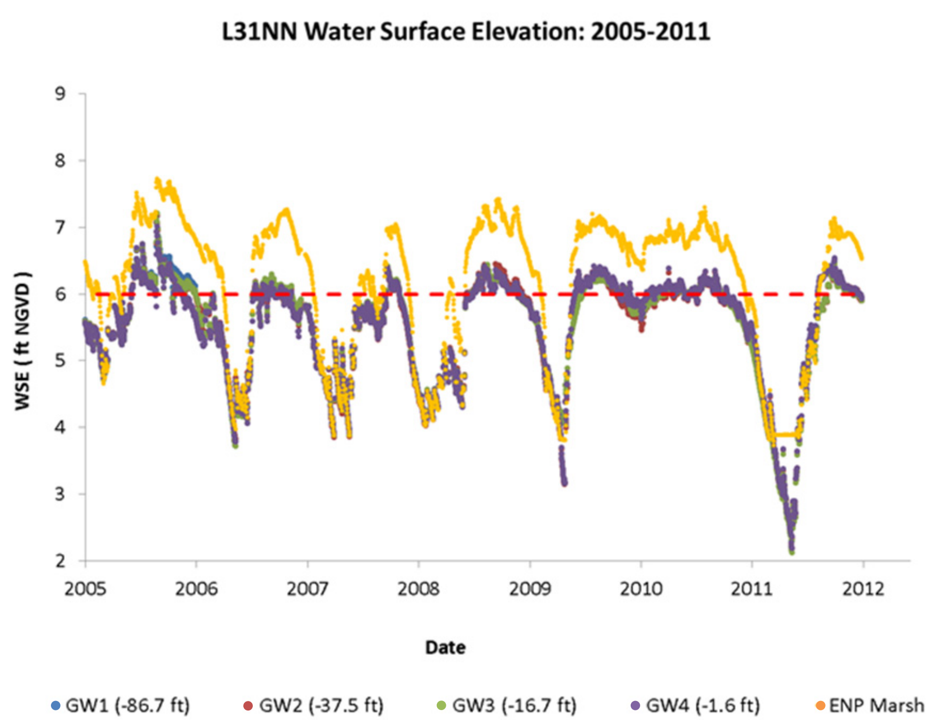

Figure 10. Water Surface Elevation at L31NN, 2004-2011. Yellow indicates surface water table; dashed red line indicates elevation of the ground surface in marsh

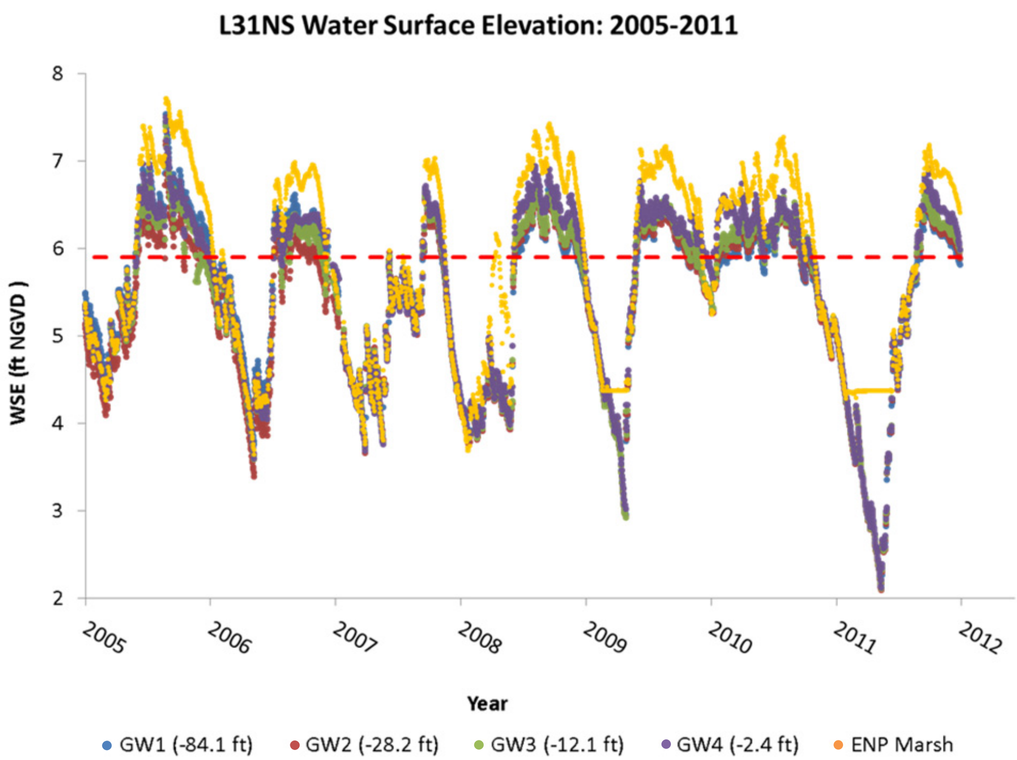

Figure 11. Water Surface Elevation at L31NS, 2004-2011. Yellow indicates surface water table; dashed red line indicates elevation of the ground surface in marsh. Elevation of center of wellscreen is given in parentheses.

While the maximum water depths and above ground water levels at the two sites are quite similar, the dry season subsurface drawdown below ground differs, appearing to occur more quickly at the southern site and drawing further below ground. These results in consistently shorter hydroperiods at the southern site (see Figure 7). In addition, the relation between surface and groundwater differs between the two sites. At the northern site, when surface water is present, the water surface elevation of the surface water is consistently approximately 1 foot higher than the groundwater water surface elevations (Figure 10). At the southern site, the surface water and groundwater heads track together much more closely, with a maximum difference of less than 0.5 feet (Figure 11).

The closer tracking of surface and groundwater at the southern site, along with the shorter hydroperiods seen there, suggest a scenario in which the underlying bedrock transmissivity at the two sites is fairly similar, but that the bedrock at the northern site may be covered by a less permeable surficial layer of soil, perhaps marl or a marl-peat mix. Under this scenario, the presence (or greater presence) at the northern site of this impeding layer may create something like a perched (surface) water table.

Elevation of water surface varied seasonally, with annual lows at the end of the dry season (March to June), and maxima during August to October, depending on the year. WSE at the L31N stations varied from 2.1 to 7.7 ft NGVD. On a given day for a well cluster, water surface elevation (WSE) tended to be highest in the deepest well (GW1), and lowest in the shallow well (GW4). The water levels (Figures 10 and 11) show sharp declines and rises as the seasons change from wet to dry. Water elevation of the L31NN surface gage tended to be higher relative to the monitoring wells during the wet season compared to the L31NS gage.

Vertical Hydraulic Gradient

The vertical hydraulic gradient (VHG) provides an indication of the direction and magnitude of head within an aquifer (see Figure 12). Groundwater tends to flow in the direction of the hydraulic gradient proportional to the head difference. A VHG of zero means there is no head difference between the piezometers.

Calculation of VHG for the north and south well clusters represents the difference between water surface elevation for the shallow (GW4-GW3), medium (GW3-GW2), and deep (GW2-GW1) wells. VHG for the full periods of measurement are shown in Figures 13 and 14. A representative detailed time series for a several month period during the wet and dry season is presented in Figure 15. Comparison of VHG with rainfall and stage (WSE) indicates a clear link between larger rainfall events and changes in VHG, especially during the wet season when the marsh is inundated (Figure 15).

At L31NN, by far the highest gradient compared to other pairings was observed between the surface water and the shallowest well (L31NN-GW4; see Figure 13B). The observed positive VHG for L31NN-GW4 suggests downward flow occurs most of the time, except when the ENP marsh is dry. The vertical gradients were greater at L31NS compared to L31NN, especially for the shallow wells (VHG4_VHG3). There was close to zero VHG between GW2 and GW1 at L31NN throughout the six-year study period. But on any given day, water levels were highest in GW1. The VHG results are complex and would benefit from further analysis. It seems clear that dissimilarities exist between L31NN and L31NS based on the trends in VHG.

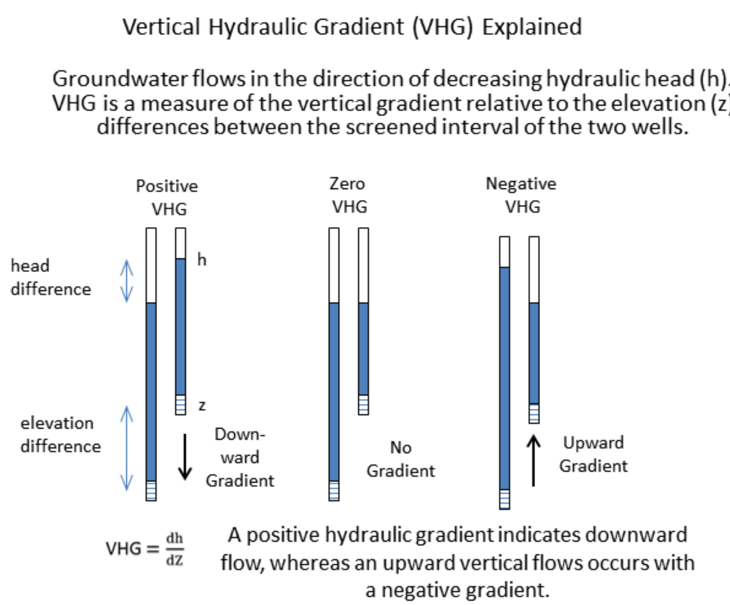

Figure 12. Explanation of vertical hydraulic gradient (VHG)

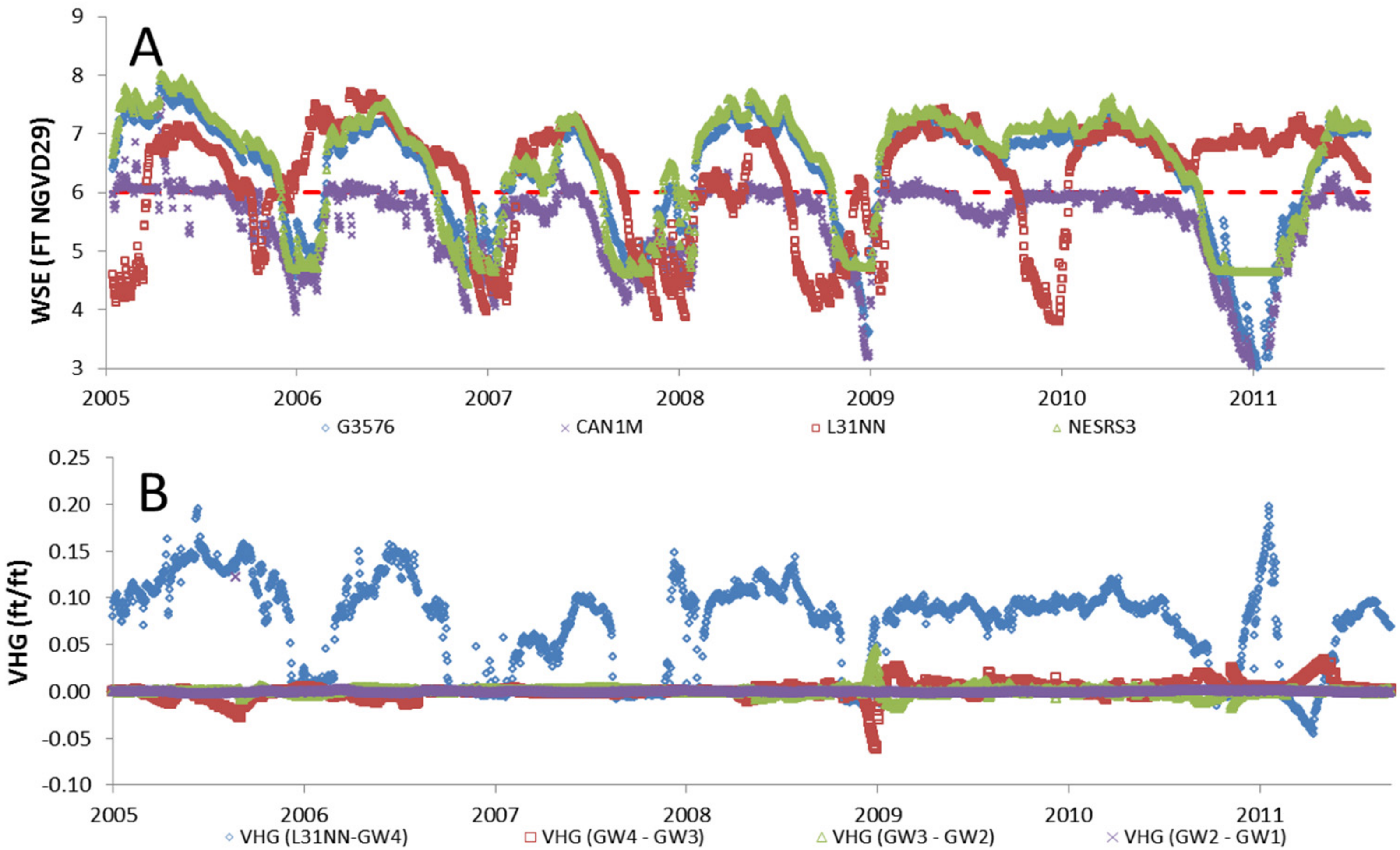

Figure 13. A. Water Surface Elevation (WSE) and B. Vertical Hydraulic Gradient (VHG) at L31NN during 2004-2011.The red dashed line represents the elevation of the ENP Marsh bed.

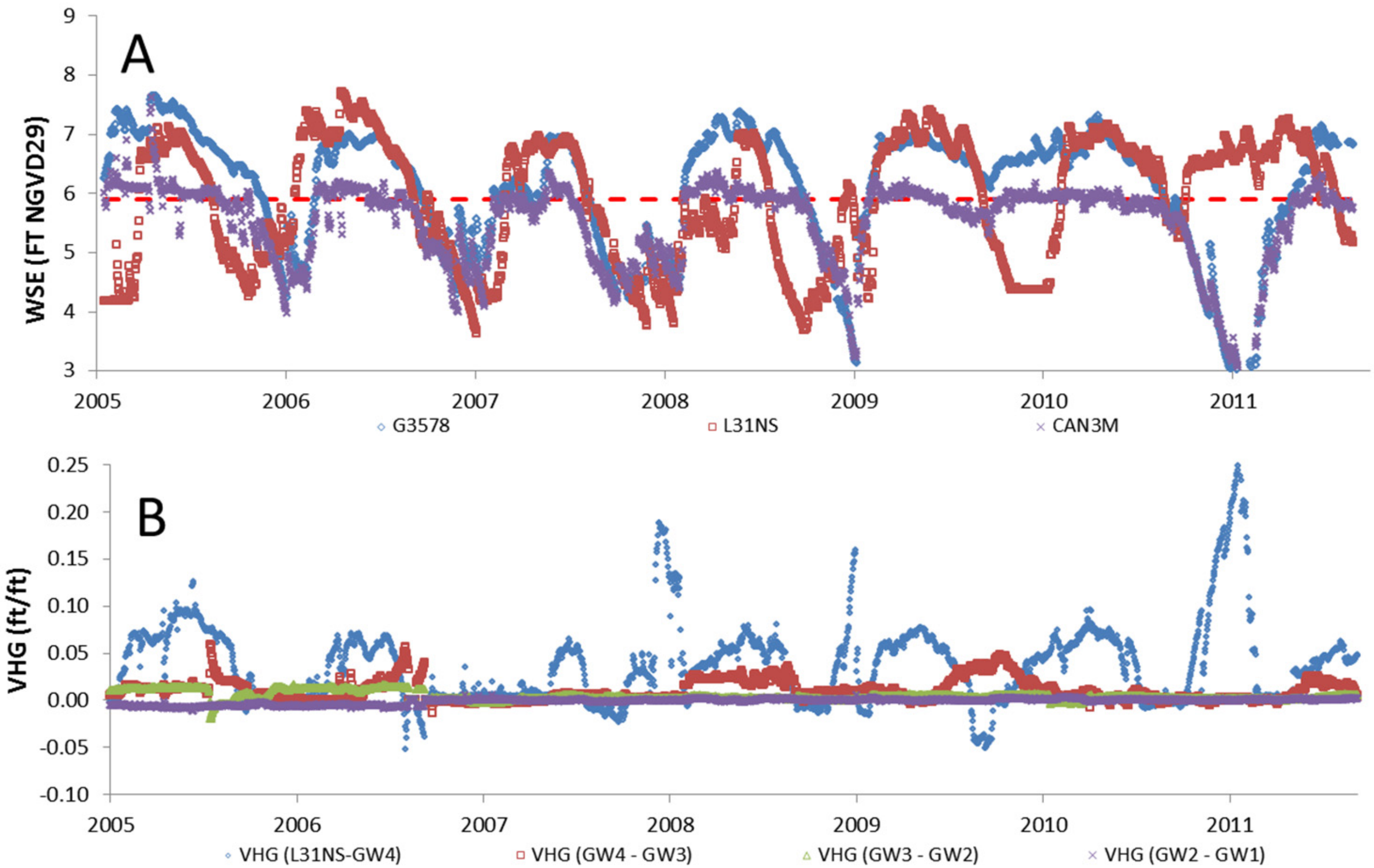

Figure 14. A. Water Surface Elevation (WSE) and B. Vertical Hydraulic Gradient at L31NS during 2004-2011. The red dashed line represents the elevation of the ENP Marsh bed.

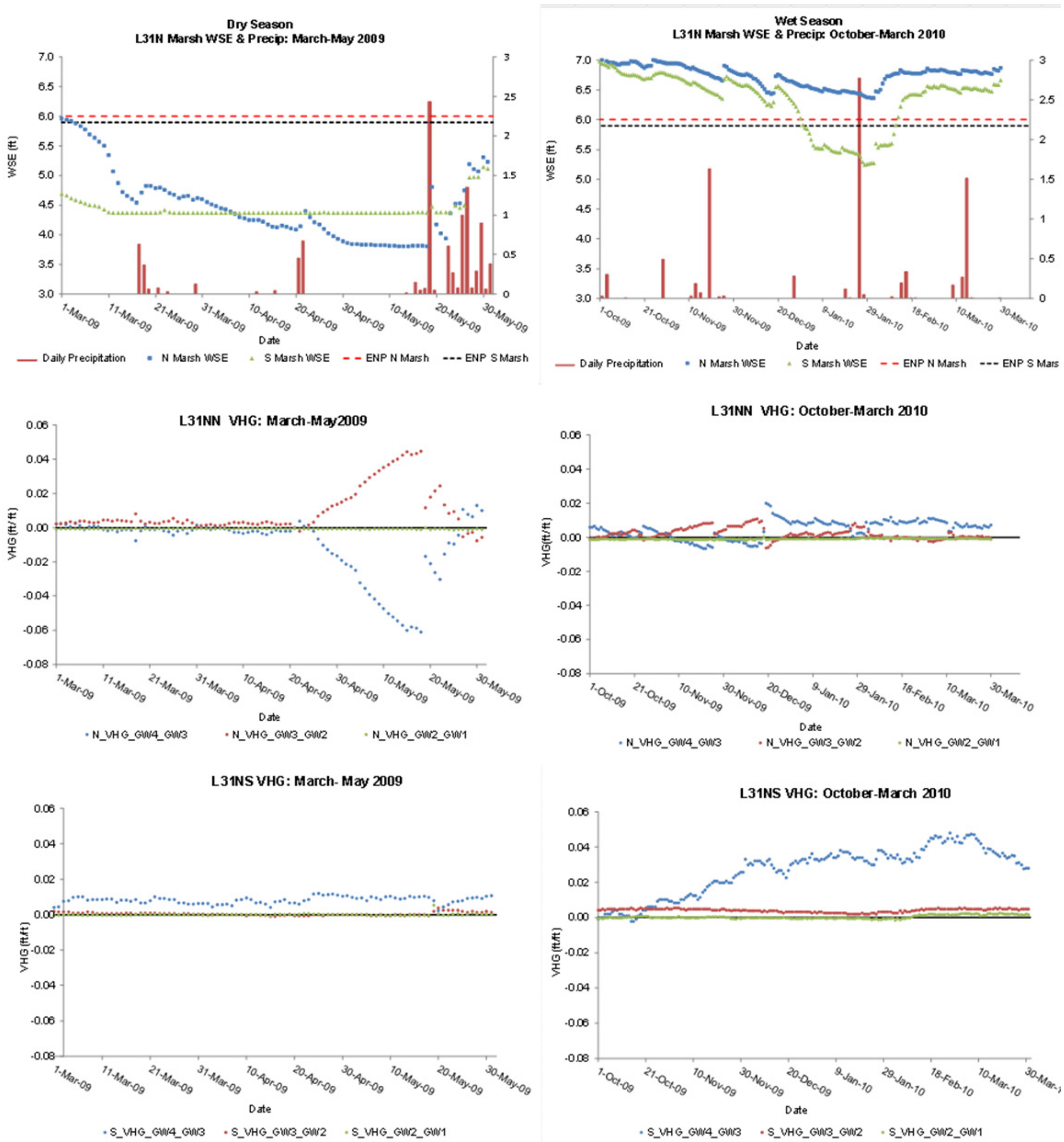

Figure 15. Marsh water surface elevation (WSE), daily precipitation at S-336, and vertical hydraulic gradient (VHG) during dry and wet season of 2009-2010.

Pumping Influences

Comparison of the WSE patterns between north and south well clusters suggests differences in hydrodynamics between the north and south stations at L31N. Contributing to the observed differences is an apparent influence from pumping of groundwater. For example during February 2005, the WSE at L31NN wells had a gradual downward trend, but showed little separation among the four wells (Figure 16). In contrast the WSE time series at L31NS possessed a distinct sawtooth pattern with a period of one day. This suggested influences of nearby pumping during some periods (Figure 17). During February 2005 the pattern was repeated on a daily basis throughout the month. During other periods, such as February 2009 the drawdown pattern was reduced to 4 or 5 days per week (Figures 18-19). The pumping influence appeared to follow a work week schedule, for example it did not occur on holidays (Brock and Krupa (2014) – Appendix D. This pumping influence did not affect the WSE of the canal, but did impact the marsh surface elevation to the west under some conditions (e.g., December 2008; Brock and Krupa (2014) – Appendix D. Furthermore, the oscillations were observed at the L31NS site, but not at L31NN (compare Figure 16 to 17 and Figure 18 to 19), suggesting the source of the drawdown is in the proximity of L31NS. It appears that the source of the groundwater oscillations is pumps that withdraw water at the Krome Quarry Plant Site, located to the east of L31NS (Figure 3; SFWMD Permit 13-00120-W). With a capacity of 18,000 gpm, these process pumps are used to wash limestone rock mined from the adjacent quarries (see Figures 2 and 3). Analytical groundwater simulation model results contained in the permit application indicated the potential for drawdown that extended to the L31NS station. This periodic pumping provides a signal that has the potential to aid in the assessment of hydrologic fluxes in this complex aquifer.

Oscillations in L31N surface and ground water elevations occurred in October-November 2010, suggesting a different pumping influence than described in the above paragraph. These oscillations, which have a periodicity of 1 day, occurred in both the L31N canal (Figure 20) and the monitoring wells at both L31NN and L31NS stations (Figure 21). The observed oscillation pattern extended up several miles to the L30 monitoring stations [Cardno ENTRIX and DRI (2011)]. These oscillations were attributed to a pumping cycle at S-332B (USACE, Personal Communication). The surface water oscillations were accompanied by an oscillation in groundwater flow velocity at L31NNGW3 (Figure 21).

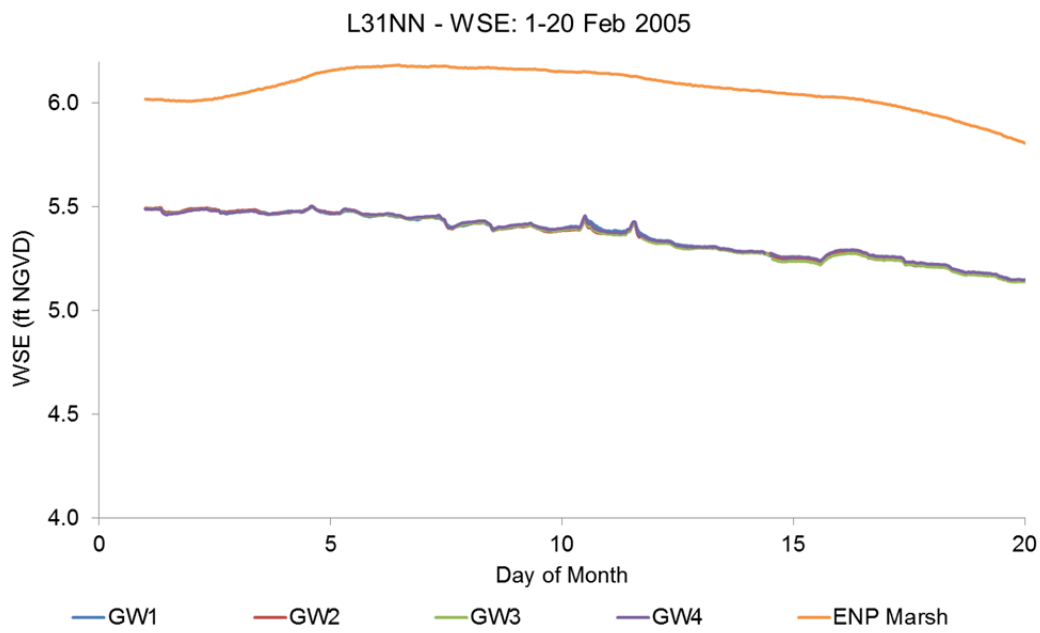

Figure 16. WSE at L31NN during 1-20 Feb 2005. Note the lack of separation in elevation among the four wells.

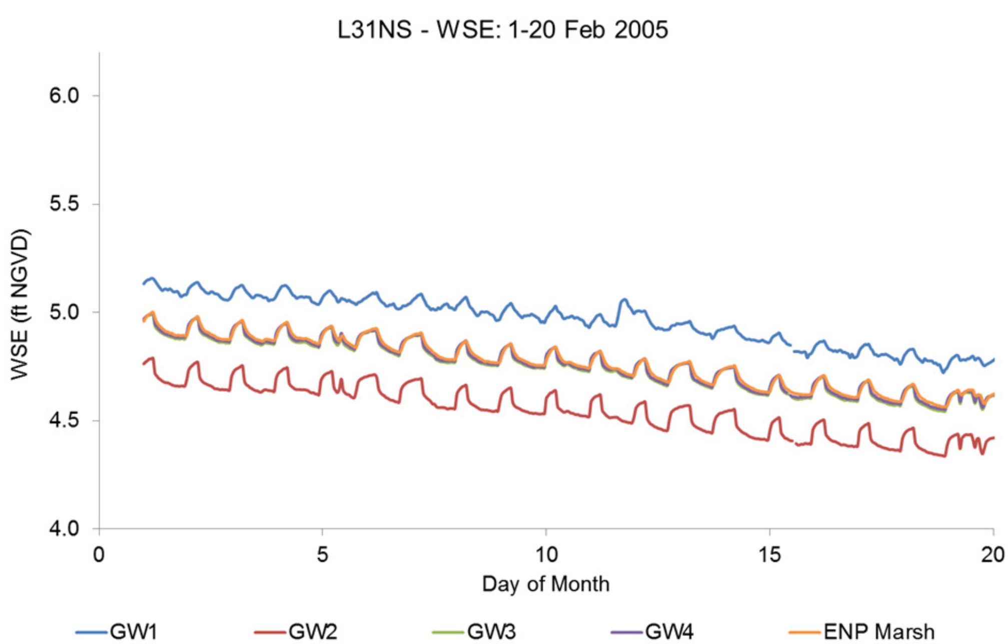

Figure 17. WSE at L31NS during 1-20 Feb 2005. Note the separation in elevation among the four wells, and the sawtooth pattern that reflects drawdown by apparent pumping seven days of the week.

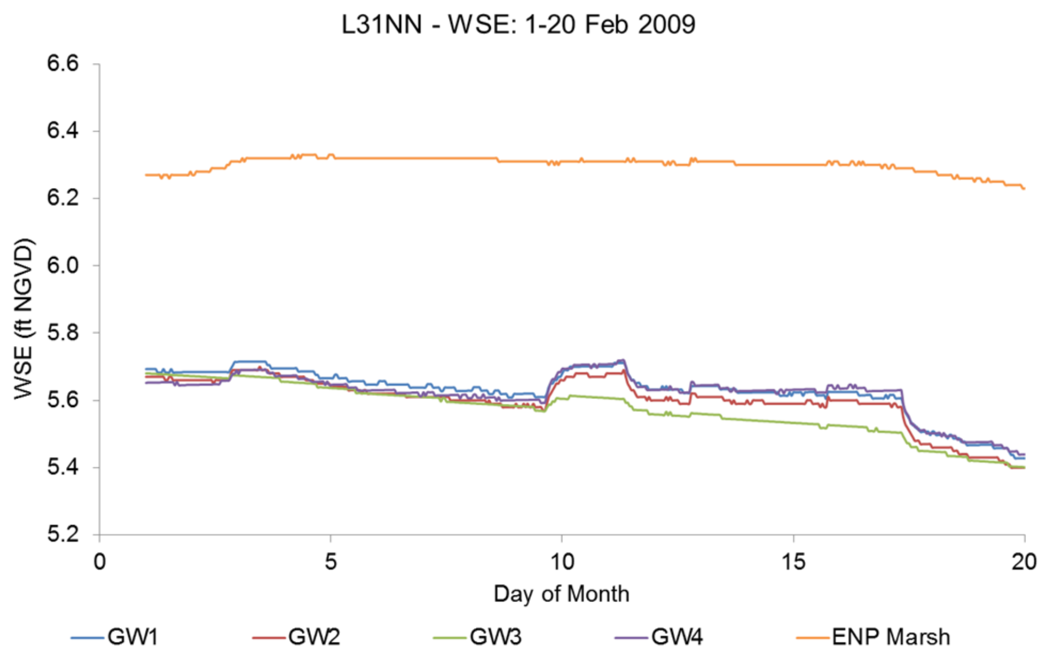

Figure 18. WSE at L31NN during 1-20 Feb 2009.

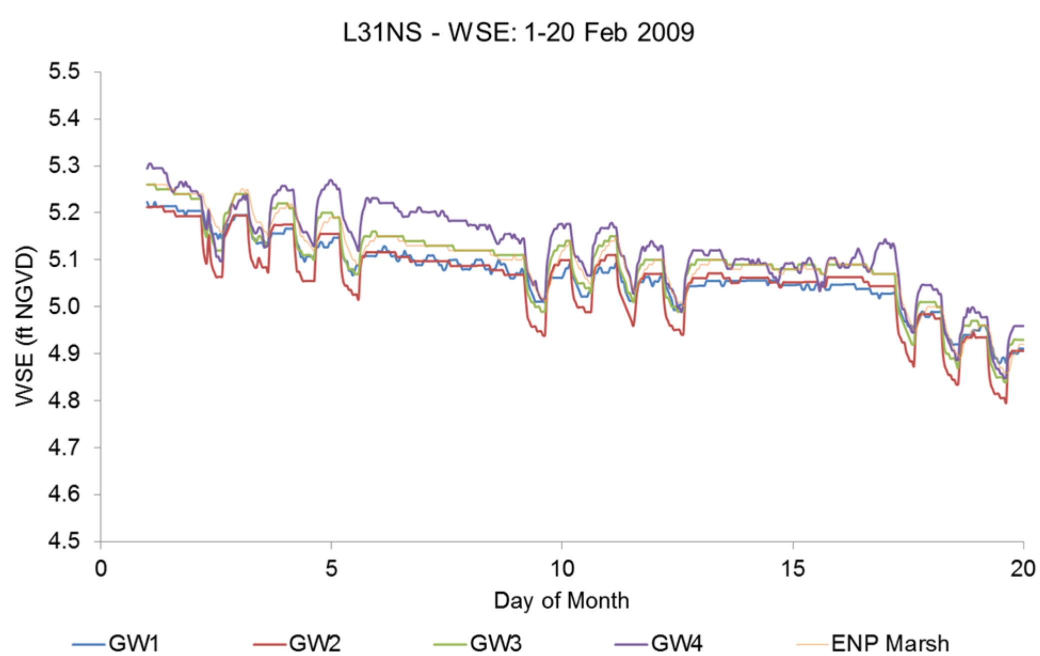

Figure 19. WSE at L31NN during 1-20 Feb 2009. Note the drawdown that occurs due to apparent pumping four days out of each week.

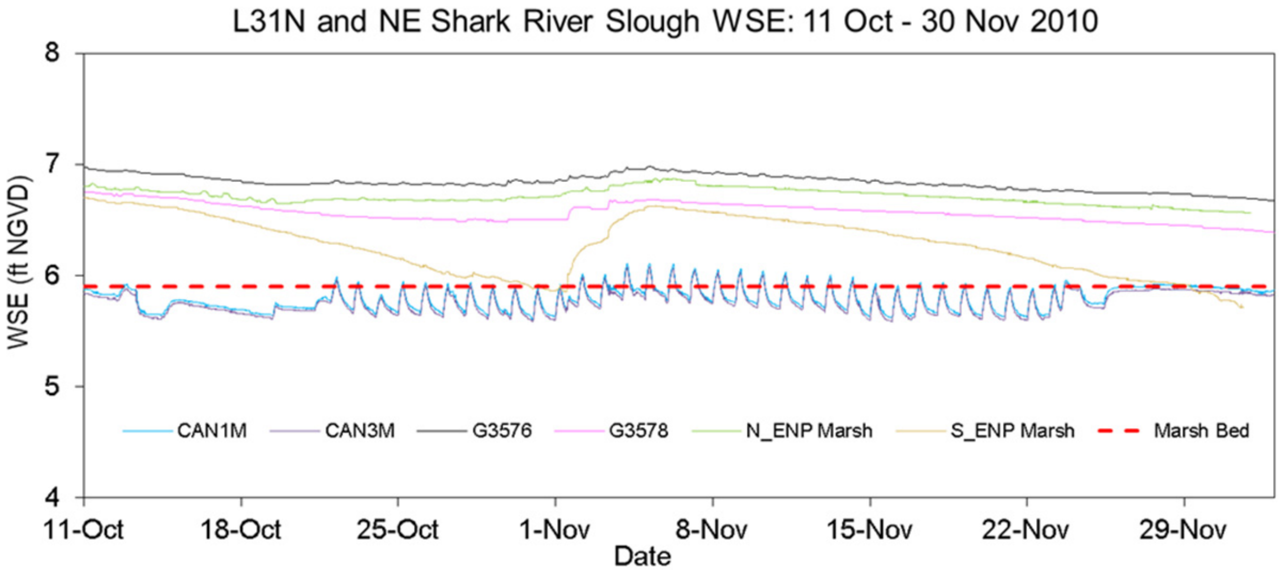

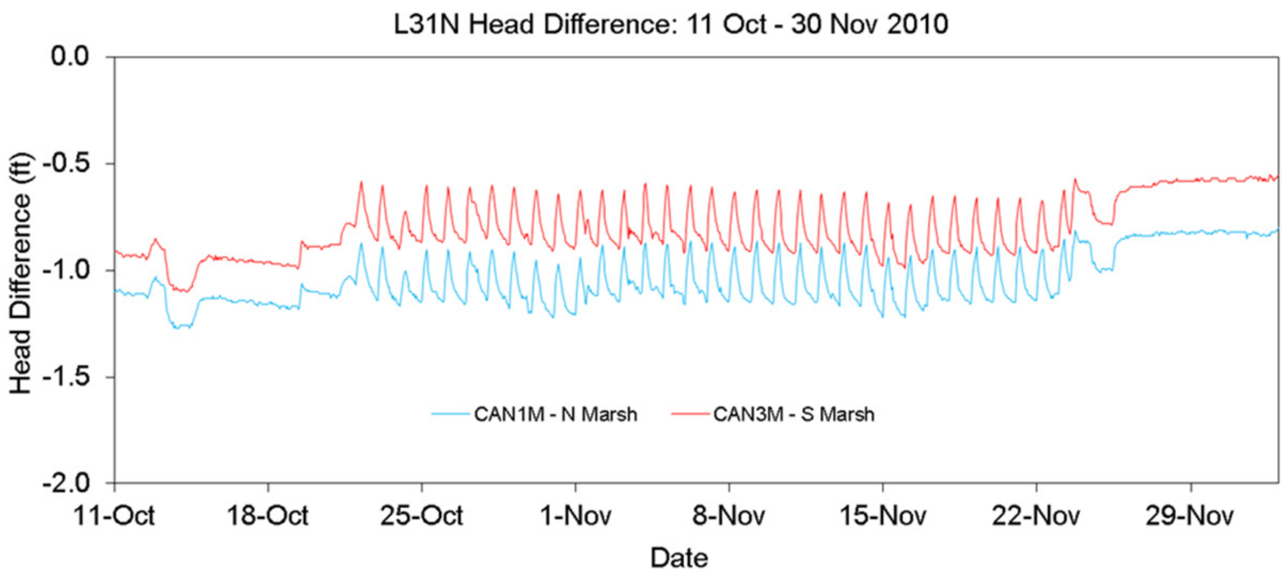

Figure 20. Water Surface Elevation (WSE; top) of L31N surface water illustrating the regular oscillations in elevation that occurred during Oct-Nov 2010. The head difference is shown (bottom) between the L31N canal and North and South marsh level stations.

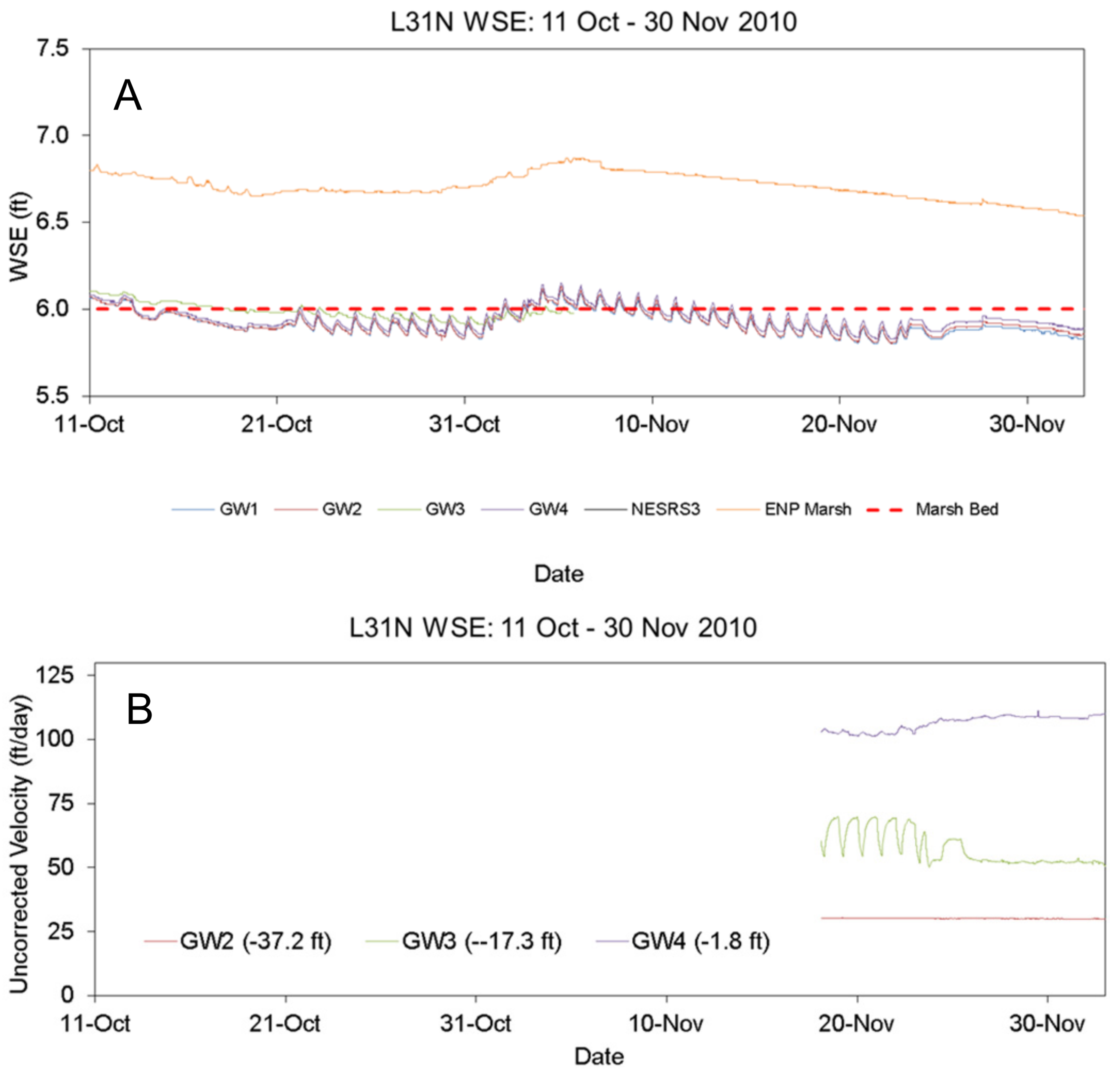

Figure 21. A. Water Surface elevation (WSE) at L31NN and B. Velocity at L31N during 11 October to 30 Novermber 2010. Velocity data are not available for the period 11 October through 18 November 2010.

Dynamic Hydraulic Threshold at L31N Aquifer

Analysis of water elevation, velocity, and temperature data for 2006-2009 suggests that a threshold head effect exerted an important control in regulating flow in the L31N portion of the Biscayne Aquifer. We hypothesize the presence of this "threshold" because there does not appear to be a 1:1 correspondence between increases in head and flow rate throughout the range of WSE observed over the entire year. The dynamic behavior of the threshold during summer through fall 2007 is illustrated for the L31NN and L31NS stations in Figure 22 and Figure 23. The flow response differed at the two stations. Surface level (green) rose above the marsh bed during late September at both the north and the south stations, but the WSE in the north groundwater wells did not rise with the surface as high in the north as it did in the south (Figure 22A and Figure 23A). The elevated head above the bed led to a substantial increase in flow velocity at the south, but not at the north. (Figure 22B and Figure 23B).

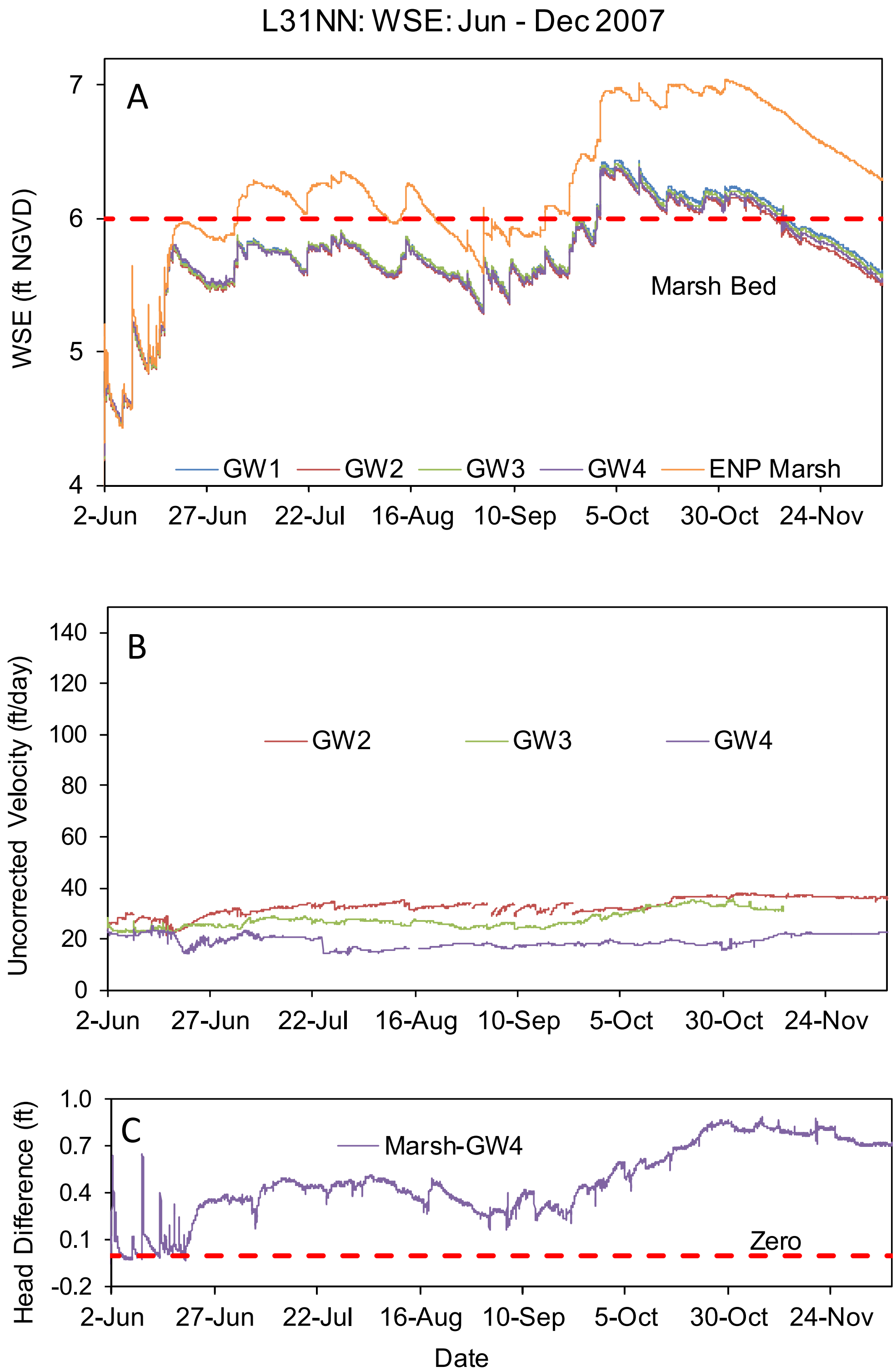

Figure 22. At L31NN, the oscillations in Water Surface Elevation (WSE; top) were associated with variation on velocity at L31NN GW3 (bottom). Velocity data from GW1 are not available for this period.

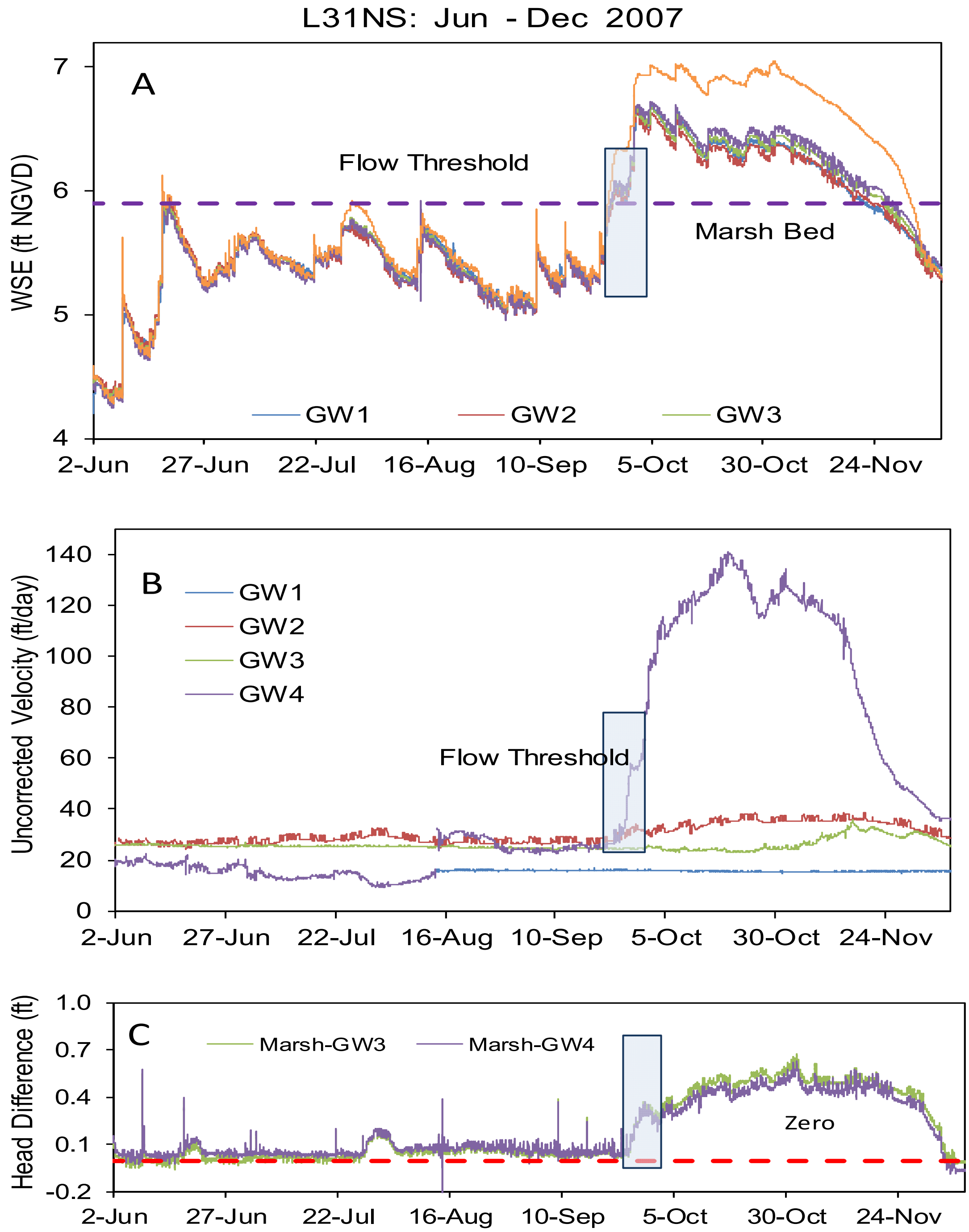

Figure 23. WSE (A) Uncorrected Velocity (B), and Head (C) for L31NS during June-December 2007. The transparent blue rectangle highlights the period when the rate of change in velocity exceeds the corresponding head difference.

Water Temperature

Time series measurements of parameters independent of the flowmeter, but responsive to flow, may be able to provide useful insight for scaling measurements from multiple depths into accurate predictions of regional groundwater flow. The aquifer monitoring program at nearby WCA3B has demonstrated that two useful "tracers" of flow are water temperature and electrical conductivity (Cardno ENTRIX and DRI 2011).

Time series measurements of water temperature were available for the L31NN and L31NS sites at three depths, the water column of the marsh (from the stilling well) and at two different depths within each of the wells, namely from the pressure transducer in the top portion of the well and from the groundwater flowmeter at the wellscreen. Table 3 shows the distribution of the depths with measured temperature time series. These data were analyzed for the period June-December 2007, allowing a contrast between periods of low groundwater flow (June-August 2007) and high groundwater flow (October-December 2007). Comparison of the time series of temperature seen in the surface water with those seen at the various depths within the aquifer is particularly illustrative. Figures 25 and 26 show the data for the two sites, arranged by well. Comparisons for the eight wells are summarized in Table 3, and reveal several patterns. As might be expected, at the -86.8 foot depth (NGVD 1929) it is clear that very little of the temporal variability in the surface water (blue trace) is translated to the 86 foot depth (panels A; green traces), either at the L31NN or L31NS sites. At the next shallower depths, -37.2 and -28.4 feet, the pattern is similar – almost completely flat with little visible connection to the surface temperature signal.

In contrast, at the shallower depths, +2.54, +2.5 and -1.8 feet NGVD 1929, the groundwater temperatures almost exactly mimic the surface water temperature, suggesting rapid flow of surface water into the upper six feet or so of the aquifer. This is a reasonably expected result.

The more surprising results are seen in the range of patterns exhibited at intermediate depths, -4.4 to -13.0 feet, NGVD 1929, and in the differences between the L31NN and L31NS sites. At these intermediate depths, some depths show very close tracking to surface water, but only for part of the time period, typically September to November. This is seen most strongly at the L31NS site, and appears to be related to the sudden onset of flow in October (Figure 24B). The conformity in temperature pattern may also be related to the apparently stronger connection between surface water and groundwater at L31NS site compared to L31NN demonstrated as shallower surface water depths and shorter hydroperiods (Figures 7, 10, and 11).

It is also striking that numerous time series available at close to -4 feet NGVD 1929 vary widely in their similarity to the surface water signal, despite all being at very similar depths. The time series at L31NS GW3 PT (-3.8 ft), at L31NS GW1 PT (-4.0 ft), L31NN GW1 PT (-4.4 ft), and at L31NN GW3 PT (-5.8 ft) all show rolling signals with no direct connection to surface water. In contrast, at L31NS GW2 PT (-4.4 ft) the thermal pattern tracked the surface water signal closely in October and November, and at L31NN GW2 PT (-4.4 ft) the signal tracked surface water closely throughout most of the year except near the end of the previous dry season. The variability in response at similar depths suggests substantial aquifer heterogeneity and presents a challenge to scaling up to the regional scale. Although the available thermal profile data are limited to only a few elevations in different wells, they suggest that temperature monitoring may provide a useful tool for tracing movement of water into and through the shallow aquifer.

Overall, time series measurements of temperature appear to be a useful supplement to flow measurements, particularly in heterogeneous aquifers. Temperature has become extensively utilized to track movement of groundwater in other aquifers (Constantz 2008). Although heat has not been used to monitor movement in the Biscayne Aquifer, these data and previous findings at L30 (Brock, unpublished data) suggest that the technique has strong potential to contribute to our understanding of groundwater movement, especially when coupled with other measurements. From a simulation modeling perspective, use of multiple parameters (e.g., pressure, temperature, groundwater flow rates, electrical conductivity) reduces the number of degrees of freedom during the parameter estimation process and thereby helps minimize uncertainties introduced by spatial heterogeneity (Naranjo et al. 2012).

Table 3. Shape and degree of match to surface water temperature time series for June-December 2007 at L31NN and L31NS.

Site and Figure No.	Panel in Figure	Depth (ft) NGVD29	Well	Temperature Sensor	Shape & degree of match to surface water temperature time series
N, Fig. 25	A, B, C, D	Ca. +6	NN	Surface	--
N, Fig. 25	D	+2.5	GW4	PT	Close track throughout
N, Fig. 25	D	-1.8	GW4	WS	Close track throughout
N, Fig. 25	A	-4.4	GW1	PT	Slight increase, but greater amplitude
N, Fig. 25	B	-4.4	GW2	PT	Close track except June
N, Fig. 25	C	-5.8	GW3	PT	Slight increase, but greater amplitude
N, Fig. 25	C	-17.3	GW3	WS	Slight increase
N, Fig. 25	B	-37.2	GW2	WS	Near flat; no tracking
N, Fig. 25	A	-86.8	GW1	WS	Flat; no tracking
S, Fig. 26	A, B, C, D	Ca. +6	NS	Surface	--
S, Fig. 26	D	+2.5	GW4	PT	Close track throughout
S, Fig. 26	D	+0.7	GW4	WS	Fairly close tracking Sep-Nov
S, Fig. 26	C	-3.8	GW3	PT	Slight increase, but greater amplitude
S, Fig. 26	A	-4.0	GW1	PT	Slight roll
S, Fig. 26	B	-4.4	GW2	PT	Fairly close tracking Oct-Nov
S, Fig. 26	C	-13.0	GW3	WS	Slight increase roll + close track Oct-Nov
S, Fig. 26	B	-28.4	GW2	WS	Mostly flat; slight roll
S, Fig. 26	A	-84.0	GW1	WS	Flat; no tracking

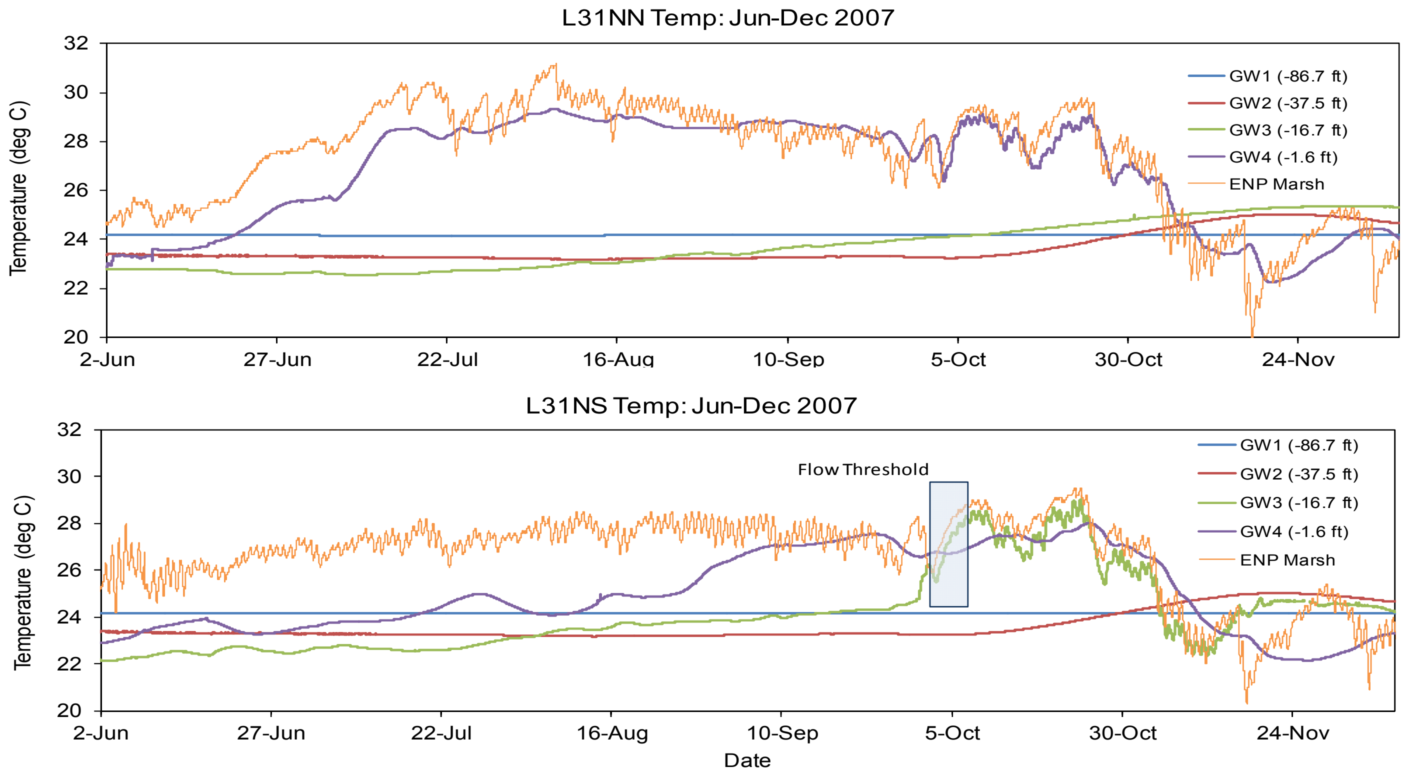

Figure 24. Temperature at the well screen for GW1-GW4 wells at L31NN and L31NS during June-December 2007. A stark difference between northern and southern site in thermal response of the shallow aquifer is shown by the bright green line, which confirms movement of water bearing a surface thermal signature down to a depth of -16.7 ft. The transparent blue rectangle highlights the period when groundwater movement in the shallow aquifer in the vicinity of L31NS appears to accelerate, leading to mixing of surface water temperature with water at an elevation of -17 ft (GW3) (see also Figure 23B). Note the difference in thermal pattern observed between the north and south stations for GW3. The shallow aquifer (down to -17 ft) in the south reached equitemperature with surface water from 5 October 2007 through November, nearly one month earlier than at the south station.

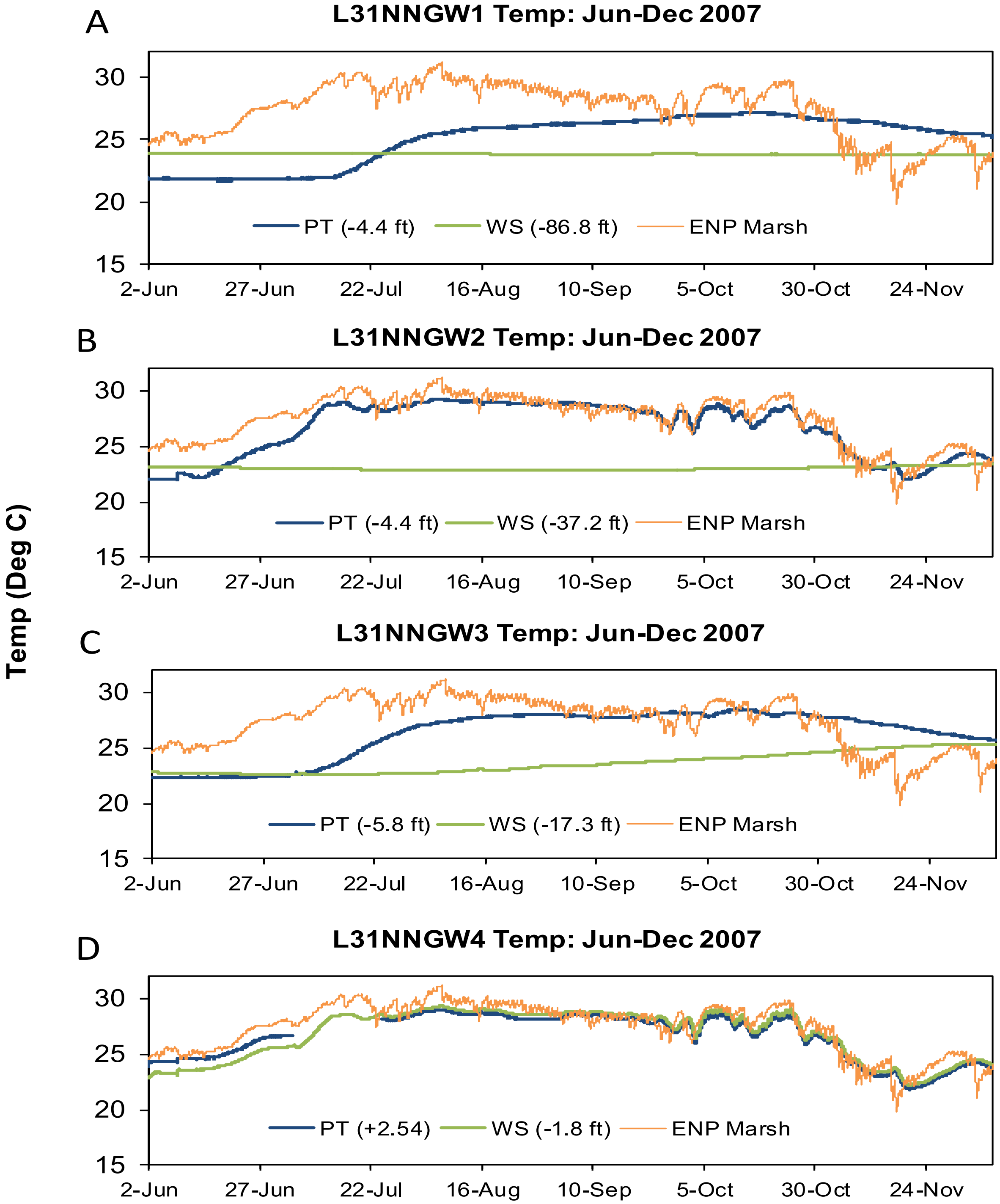

Figure 25. Water temperatures at the L31NN site: Marsh Bed (Surface water) and at two different elevations in each of the four wells: "Pressure Transducer (PT)" and "Well Screen (WS)." June-December 2007. The actual elevation (NGVD 1929) of the well temperature is given in parentheses.

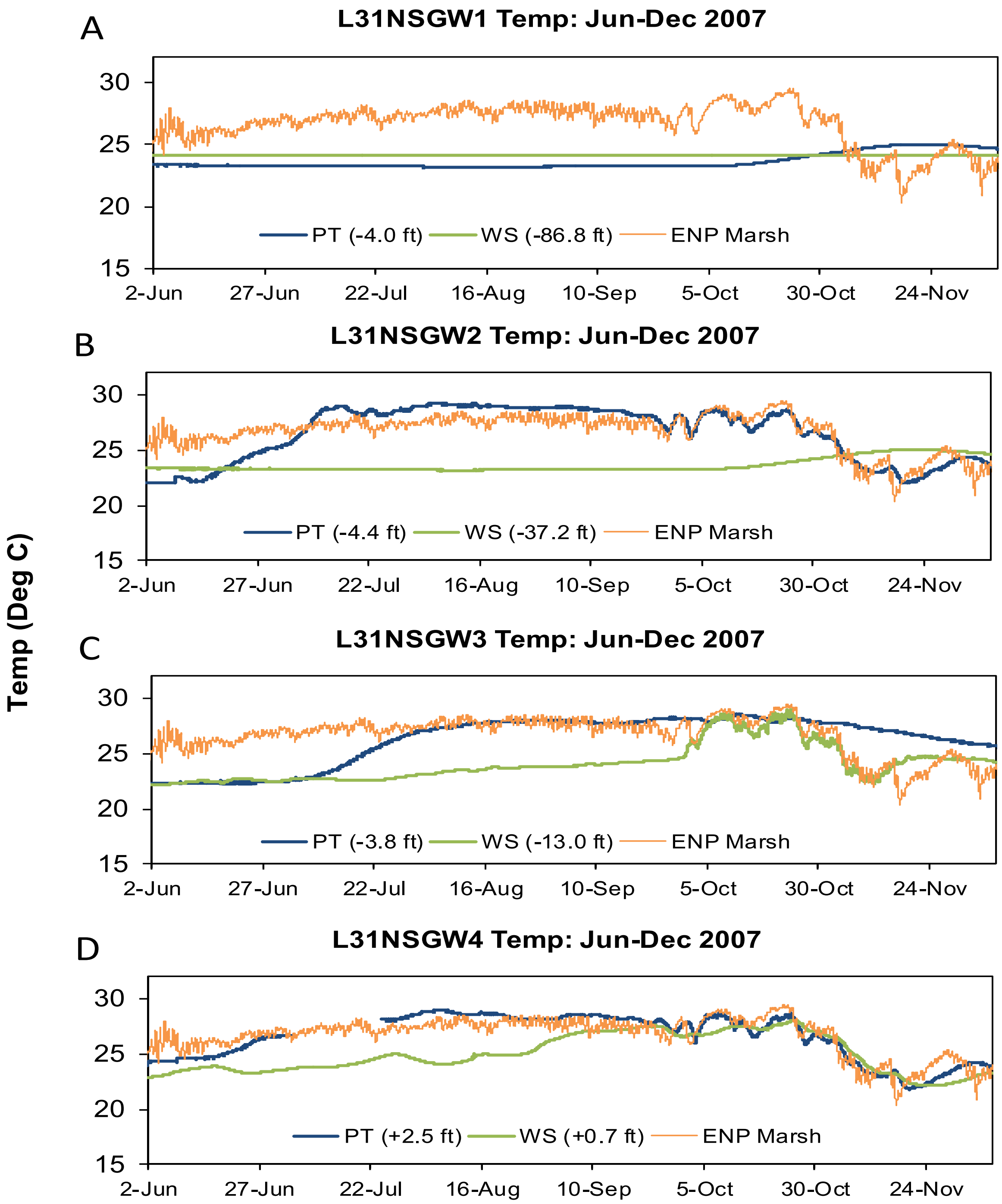

Figure 26. Water temperatures at the L31NS site: Marsh Bed (Surface water) and at two different elevations in each of the four wells: "Pressure Transducer (PT)" and "Well Screen (WS)." June-December 2007. The actual elevation (NGVD 1929) of the well temperature sensors is given in parentheses.

Heat Pulse Flowmeter Performance

This study represents the first known application of multiple groundwater flowmeters operated over a multi-year period. As this was a pioneering application of the instrumentation, we experienced some problems and encountered issues that led to revisions to the equipment and procedures during the project. Some of the problems and remedies are summarized in Table 4.

Table 4. Instrument and methodological issues encountered in the L31N study

Issue	Description	Remedy
suspension rod failure	clips connecting rods became corroded over time (2+ years)	replaced plated steel hardware with stainless steel
thermistor failure	thermistors failed to function properly	replaced original thermistors with an alternative manufacturer
failed heat pulse probe requires repair	original probes had soldered internal connections between thermistors and connector	replace soldered connections with a screw terminal circuit board
conflicts with other well users	other users of the wells removed and replaced rods backwards	communication with other agencies about the flowmeters
sedimentation	sediment accumulated in well	Performed periodic redevelopment of wells
vertical flow variability within well screen	large variability in velocity	measured velocity profile and selected highest velocity for probe placement
cramped vaults	wellhead vaults have limited space for multiple sensors	recommended larger vaults for new well construction
poor drainage of wellhead	rainwater pools in vault and can run down conduit and enter instrument enclosure	recommended better drainage for new well construction

Issues such as those presented in Table 4 led to periods where the performance of the heat pulse flowmeter was outside of normal operating specification. Such periods of abnormal behavior of the instrumentation can be identified using diagnostic procedures involving the thermal response of the probe during the heat pulse cycle. Data were deleted in the course of the quality assurance review during such periods of probe failure.

Results of groundwater velocity and flow direction for the eight flowmeters are presented in Figures D3 to Figure D18. Velocity data in some wells appear erratic, for example L31NNGW1. The flowmeter performance in other wells during other periods appears credible, for instance L31NS during June-November 2007 (Figures 23 and D17).

Water flow direction at the L31N stations generally trended towards the east and south, and varied seasonally, more so in the shallower wells (Figure D10 and Figure D18). Change in flow direction of the south shallow aquifer seemed to respond to periods of increased head, for example during spring 2008, when the flow azimuth (direction to which the water flowed) changed from south (170 degrees) to south west (270 degrees). A suggested area for future data analysis is the relation between seasonal changes in flow direction and vertical hydraulic gradient.

FINDINGS

When constructed in 2005, the L31NN and L31NS stations were the first groundwater monitoring sites in South Florida specifically designed to measure velocity and direction of water movement. The design of the stations with co-deployed pressure transducers and groundwater flowmeters in a single well standpipe proved to be a valuable approach; however, limited space within the two inch casing suggested that a four-inch diameter casing would have been preferable. Installation of four-inch diameter wells would accommodate temperature and electrical conductivity sensors in addition to the presently installed pressure transducer and groundwater flowmeter. Additionally, performance of flowmeters in the laboratory calibration tank suggested that use of a stainless steel V-rib well screen would have been preferable to the two-inch, slotted PVC well screens. Our experience suggests that four-inch diameter stainless steel screens are to be recommended for future well construction for use with heat pulse flowmeters and supplemental probes. This suggestion is supported by Bayless et al. (2008), who evaluated flowmeter performance and reported that the most accurate results for velocity and direction were obtained with four inch stainless steel wire wrapped screens (compared to two inch PVC wellscreens).

Vertical strings of temperature or conductivity sensors would be very helpful for quantifying aquifer heterogeneity. An array of sensors spaced vertically a few feet apart and extending from the surface down to the lowest wellscreen (about -80 feet) would closely match the scale of known macroporosity. Time series measurements from the array would indicate how and whether the macroporosity translates into flow variability.

SUMMARY AND CONCLUSIONS

Groundwater flow rates in the karst bedrock of southern Florida are highly variable but can be locally significant due to the high transmissivity of the Biscayne Aquifer. Seepage tends to concentrate in preferential flow zones with carbonate strata with permeability that extends horizontally over great distances. This large flow volume has suggested that seepage control measures (e.g., engineered cutoff walls with low permeability) might provide an effective means for regional flow management.

While flow dynamics appear to be complex in this aquifer, the heat pulse groundwater flowmeter produced credible velocity and flow direction data.

This project provided an unprecedented multiyear time series of groundwater flow and achieved the project objective of adapting an instrument intended for short term installations for long term unattended use. The long-term reliability of thermistors was an issue, and underscored the value of monitoring instrument performance by wireless telemetry. Some problems due to sediment accumulation in the wells were also noted, leading to our recommendation that a sump of at least 2.5 ft beneath the screened interval of the well be present.

Review of data from the L31N monitoring well stations indicated that hydrologic conditions were highly variable over the 7-year period ending in 2011. Measured flow velocities varied non-randomly over time. While comprehensive explanation of the observed temporal variability will require additional study, sufficient data were collected to suggest the controlling processes. Local conditions of hydraulic gradient appeared to drive the observed groundwater flow rates. The groundwater velocities responded quickly (within an hour) to variations in hydraulic head associated with changes in canal elevation as well as apparent aquifer drawdown from industrial pumping activity.

Spatial heterogeneity of the Biscayne aquifer remains a complication, as does the issue of upscaling from groundwater well-based point measurements to regional flow. While acknowledging the limitations placed on point measurements by spatial variability, we at the same time emphasize that the spatial limitations do not appear to diminish the strength of the time series measurements made at specific points. Stated differently, while flow recorded by a flowmeter at a particular point within the aquifer may or may not be representative of the aquifer as a whole, the time series can be a very strong source of information, particularly if there are distinctly shaped temporal signals that can be related to time series of driving forces. We encourage the exploration of supplemental networks of proxy measurements (e.g., electrical conductivity and temperature) that have sufficiently low cost to allow large numbers of sensors to be installed in wells. Such large numbers of sensors, each generating long term time series may prove to be an important method for addressing spatial variability and quantitative upscaling.

Changes in flow velocity in some wells were thought to be related to nearby pumping. We recommend learning more about the timing and magnitudes of pumping activity that occurs to the east of L31NS. It may prove possible to use the monitoring wells and pumping activities to determine aquifer characteristics.

This study has illustrated the complexity of flow dynamics in the Biscayne aquifer. Groundwater flow rates can be substantial during time periods when the hydraulic gradient is sufficient. Evaluation of the effectiveness of seepage management measures would best include conditions that span the hydrologic extremes and employ multiple assessment tools.

The monitoring project at L31NN and L31NS has led us to the following conclusions:

- Heat Pulse Flow meters are able to detect flow, including magnitude and direction with a high degree of repeatability
- Both flow velocity and direction were affected greatly by the placement of the probes within the well screen.
- Heat Pulse Flowmeters are able to endure long (multi-year) field deployments and successfully produce consistent data, provided the instruments are serviced periodically.
- Reliability of Heat Pulse Flow meter instrumentation has improved with advancements in data acquisition systems and manufacturing. The technology has proven most reliable when sufficient time and attention can be applied to tuning and maintaining the measurement systems. The most common long term reliability issues encountered was associated with water intrusion of probe connectors that lead to failure of thermistor measurements.

- We have learned that probe-to-probe variation can be significant, and the measurement systems can be tuned to better match low or high range flow conditions.
- Heat Pulse Flow meters—in the existing L31NN and L31NS instrumentations--can be remotely monitored to ensure data QC.
- Proper monitoring well construction including attention to appropriate well screens and filter packs is essential for collection of consistent flow in a macroporous, vughed media like the Miami Oolite.
- Water stage and vertical head gradient data based on long established measurement technology indicate that flows through this aquifer are more complex than through uniform porous media.
- Flows are primarily to the East, ranging from NE to S.
- Flow velocity magnitudes are generally <5 to 150 ft/day.
- The magnitude of flow velocity varies over time in systematic ways related to rainfall, aquifer head, and head variations due to pumping activities.
- A change in the flow regime seems to consistently appear around the time that the water table crosses (rises above or falls below) the ground surface within ENP.
- Use of multiple parameters (flow, temperature profiles, stage, gradients, electrical conductivity) helps to provide a more complete picture of flow dynamics over time and space. This is especially true in an aquifer with this very high level of heterogeneity.
- The presence of an increase in head does not lead to an increase in flow rates. One cannot infer flow velocity (seepage) changes from measurements of head alone.

REFERENCES

Bayless, E.R. 2008. Construction and use of a fractured-rock simulator to test horizontal borehole flow-measuring technologies. Miscellaneous Topics in Modeling and Geophysics. USGS Scientific Investigations Report 2008-5023, p. 105.

Brock, J.T. and S.L. Krupa. 2014.. Application of Horizontal Heat Pulse Flowmeter to Long Term Monitoring of Hydrological Flux in Biscayne Aquifer, Miami-Dade, Florida. Manuscript in preparation.

Cardno ENTRIX and DRI. 2011. Data Summary Report (2009 – 2011), L-31N (L-30) SMPP Baseline Hydrogeologic Testing Project Miami-Dade County, Florida. USACE Contract No. W912EP-06-D-0015 Task Order 0006 November 2011. Prepared for U.S. Army Corps of Engineers, Jacksonville District. Prepared by Cardno ENTRIX (Fort Myers, FL) and Desert Research Institute (Reno, NV).

Constantz, J. 2008. Heat as a tracer to determine streambed water exchanges, Water Resour. Res., 44, W00D10, doi:10.1029/2008WR006996.

Cunningham, K.J., R.A. Renken, M.A. Wacker, M.R. Zygnerski, E. Robinson, A.M. Shapiro, and G.L. Wingard. 2006. Application of carbonate cyclostratigraphy and borehole geophysics to delineate porosity and preferential flow in the karst limestone of the Biscayne aquifer, SE Florida, in Harmon, R.S., and Wicks, C., eds., Perspectives on karst geomorphology, hydrology, and geochemistry—A tribute volume to Derek C. Ford and William B. White: Geological Society of America Special Paper 404, p. 191-208, doi:10.1130/2006.2404(16).

Cunningham, K.J., M. C. Sukop, H. Huang, P.F Alvarez, H.A. Curran, R.A. Renken, and J.F. Dixon. 2009. Prominence of ichnologically influenced macroporosity in the karst Biscayne aquifer: Stratiform "super-K" zones. *Geological Society of America Bulletin* 121(1/2):164-180; doi:10.1130/B26392.1.

DiFrenna, V.J., R.M.Price, and M.R Savabi. 2007. Identification of a hydrodynamic threshold in karst rocks from the Biscayne Aquifer, south Florida, USA. *Hydrogeology Journal* 16:31-42.

Drost, W.D., D. Klotz, A. Koch, H.Moser, F. Neumaier, and W. Ravers. 1968. Point dilution methods of investigating ground-water flow by means of radioisotopes. *Water Resources Research* 4:125-146.

Guaraglia, D.O. and J.L. Pousa. 2006. Decreasing measuring errors of a thermal groundwater flowmeter. *Journal of Irrigation and Drainage Engineering* 132:284-287.

Guthrie, M. 1986. Use of a geo flowmeter for the determination of ground water flow direction. *Ground Water Monitoring Review* 6:81-86.

Kerfoot, W.B. 1982. Comparison of 2-D and 3-D ground-water flowmeter probes in fully-penetrating monitoring wells. Pp 264-268 in Proceedings of the Second National Symposium on Aquifer Restoration and Ground Water Monitoring. Water Well Publishing Co., Worthington Ohio.

Kerfoot, W.B. and V.A. Massard. 1985. Monitoring well screen influences on direct flowmeter measurements. *Ground Water Monitoring Review* 5(4):74-77.

Kerfoot, W.B. 1988. Monitoring Well Construction, and Recommended Procedures for Direct Ground-Water Flow Measurements Using a Heat-Pulsing Flowmeter. Pp. 146-161 in Ground-Water Contamination: Field Methods, ASTM STP 963, A.G. Collins and A. I. Johnson, Eds., American Society for Testing and Materials, Philadelphia, 1988,.

Kushlan, J.A. 1990. Freshwater marshes. Pages 324-253 in R.L. Myers and J.J. Ewel,eds. Ecosystems of Florida. University of Central Florida Press; Orlando, Florida.

Krupa, S.L., S. Hill, and C. Bevier. 2001. Miami-Dade County Northwest Wellfield Groundwater Velocity Investigation. Technical Publication WS-1, South Florida Water Management District, West Palm Beach, Florida.

McVoy, C.W., W.P. Said, J. Obeysekera, J. VanArman, and T. Dreschel. 2011. Landscapes and Hydrology of the Predrainage Everglades. Univ Presses of Florida: Gainesville, Florida. 342 pp.

Melville, J.G., F.J. Molz, and O. Guven. 1985. Laboratory investigation and analysis of a groundwater flowmeter. *Groundwater* 23:486-495.

Naranjo, R.C., R.G. Niswonger, M. Stone, C. Davis, and A.Mckay. 2012. The use of multiobjective calibration and regiona:l sensitivity analysis in simulating hyporheic exchange. *Water Resources Research* DOI: 10.1029/2011WR011179

Parr, A.D., F.J. Molz, and J.G. Melville. 1983. Field determination of aquifer thermal energy storage parameters. *Ground Water* 21:22-35.

Sisodia, S. and O.J. Helweg. 1998. Modeling the heat sense flowmeter. *J. Irrig Drain Eng*. 124:148-151.

SFWMD 2006. QA/QC of Groundwater Level Data Procedures. Procedure Q205. SCADA & Hydro Data Management Department Operations & Hydro Data Management Division. Quality Assurance/Quality Control Section

Wilson, J.T., W.A. Mandell, F.L. Paillet, E.R. Bayless, R.T. Hanson, P.M. Kearl, W.B. Kerfoot, M.W. Newhouse, and W.H. Pedler. 2001. An evaluation of borehole flowmeters used to measure horizontal ground-water flow in limestones of Indiana, Kentucky, and Tennessee. WRI2001-4139

APPENDIX A. CALCULATION OF VECTOR MAGNITUDE AND ANGLE OF FLOW

The temperature difference between the two sensors on a given axis depends on the projection of the water velocity vector onto each of the four axes. The velocity vector is found by adding its components along every axis. The sign convention used is that positive is the direction water is flowing. The magnitude of flow (V_c) and angle of flow (θ) is determined through a vector analysis of the differential temperature data along each of the four axes (N-S, NE-SW, E-W, and SE-NW). The procedure follows:

1) The conventions used in the calculation of water flow are provided in Table A1.

Table A1. The trigonometric values associated with differential temperature data used in vector analysis of water flow direction.

Direction of Water Flow	Variable Name Sign Convention	θ	sin (θ)	cos(θ)
from S to N	N_S_mV =(+)	0	0.000	1.000
from SW to NE	NE_SW_mV =(+)	45	0.707	0.707
from W to E	E_W_mV =(+)	90	1.000	0.000
from NW to SE	SE_NW_mV =(+)	135	0.707	-0.707
from N to S	N_S_mV =(-)	180	0.000	-1.000
from NE to SW	NE_SW_mV =(-)	225	-0.707	-0.707
from E to W	E_W_mV =(-)	270	-1.000	0.000
from SE to NW	SE_NW_mV =(-)	315	-0.707	0.707
from S to N	N_S_mV =(+)	250	0.000	1.000

Notes:
[1] θ measured in degrees clockwise from N

2) The x-component of each of the four vectors is determined:

x-component N_S vector = N_Sx = N_S_mV*SIN(Radians(0)
x-component NE_SW vector = NE_SWx = NE_SW_mV*SIN(Radians(45)
x-component E_W vector = E_Wx = E_W_mV*SIN(Radians(90)
x-component SE_NW vector = SE_NWx = SE_NW_mV*SIN(Radians(135)

3) The y-component of each of the four vectors is determined:

y-component N_S vector = N_Sy = N_S_mV*COS(Radians(0)
y-component NE_SW vector = NE_SWy = NE_SW_mV*COS(Radians(45)
y-component E_W vector = E_Wy = E_W_mV*COS(Radians(90)
y-component SE_NW vector = SE_NWy = SE_NW_mV*COS(Radians(135)

4) The x-components and y-components are summed:

sumx = N_Sx + NE_SWx + E_Wx + SE_NWx
sumy = N_Sy + NE_SWy + E_Wy + SE_NWy

5) The resultant velocity vector magnitude (V_c) is the square root of the sum of the square of the x and y components:

$$V_c = \sqrt{sum_x^{\,2} + sum_y^{\,2}}$$

6) The quadrant of the resultant vector is determined using the conventions indicated below:

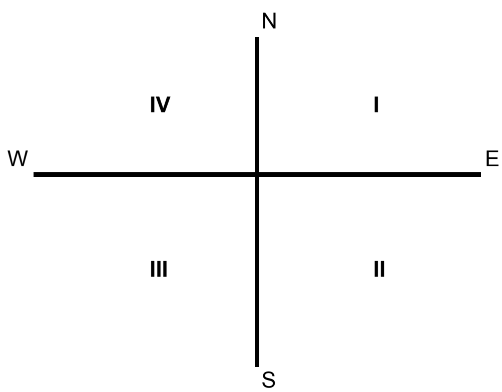

		If X sum sign is:	
		Pos	Neg
If Y sum sign is:	Pos	I	IV
	Neg	II	III

The quadrant (Q_n) of the resultant vector (I, II, III, or IV) is determined as follows:

Q_n = IF(sum_x>0,IF(sum_y>0,"I","II"),IF(sum_y <0,"III","IV"))

The resultant θ is calculated as follows:

θ =

IF(Q_n="I",DEGREES(ATAN(sum_x/sum_y)),IF(Q_n="II",DEGREES(ATAN(sum_x/sum_y))
+180,IF(Q_n="III",DEGREES(ATAN(sum_x/sum_y))+180,DEGREES(ATAN(sum_x/sum_y))
+250)))

The procedure described above represents the equations as coded for use in Excel worksheets. These equations were coded using Campbell Scientific EDLOG software to allow calculation of magnitude and direction of groundwater movement in real time using the CR23X datalogger.

APPENDIX B. CALIBRATION PROCEDURE FOR MODEL 204 PROBES

1. The probe was placed into the calibration chamber, salinity adjusted to site conditions (0.37 ppt) and temperature brought to 25 C. Two types of well screen and filter pack combinations were included to represent the conditions at the L-31N wells (see Table A1 and Table B1).

Table B1. Characteristics of the well screen and sand pack used in calibration of flowmeters to conditions at L31N.

Type	Screen Slot Size (in)	Sand Pack at Screen Interval	Porosity
A	0.01	6/20 coarse sand	0.162
B	0.06	1/4” x 1/8” pea gravel	0.420

2. The calibration software program was set for a 30 or 60 minute measurement cycle, repeated for each flow rate over a four-hour period. The first cycle was considered the stabilization period and was discarded prior to analysis, thus yielding three replicates for each flow rate. Figures 6 and 7 provide an example of temperature data collected over the course of a day during a calibration sequence. Absolute temperature data are provided for one sensor on each of four axes and differential temperature data are provided based on the pair of thermistors for each of the four axes.

2. Flow rates for the calibrations ranged between 0 and 150 ft/day. Flow rates were calculated based on the principal of flow continuity (discharge = velocity times the cross-sectional area) based on the assumption that rate of flow through the calibration chamber is uniformly distributed over its cross sectional area. The velocity was calculated as follows: velocity (ft/da) = pump discharge (mL/min) X 0.146/porosity. The 0.146 factor provides for units conversion taking into account the cross-sectional area of the chamber (182.3 cm^2) and the number of minutes in a day (1440 min/da). Typical pump discharge and corresponding velocities for the Type B Sand Pack-Filter Screen wells are given in Table B2.

Table B2. Pump discharge in the calibration chamber and calculated velocities.

Discharge (mL/min)	Velocity (ft/da)
26.45	9.19
110.8	38.5
207.3	72.0
309.5	107.5

APPENDIX C. L-31N GROUNDWATER FLOW DATA (MIAMI-DADE COUNTY, FLORIDA) FOR 2006-2009 DRI QA/QC PROCEDURES

I. Introduction

Two monitoring stations located along the L-31N Canal south of Tamiami Trail (Miami-Dade County, Florida) were equipped with groundwater flow monitoring instruments in 2006. Both of these stations (L31NN and L31NS) have five wells, one on the surface in the marsh of Everglades National Park, and four two-inch monitoring wells that are screened at various intervals of the Biscayne Aquifer to a maximum depth of 104 ft below ground surface. Each well has a pressure transducer that is operated and maintained by the South Florida Water Management District (SFWMD). Heat pulse groundwater flow meters are positioned within the well's screened interval by suspension rods. The groundwater flow meters are connected to an electronics package that is controlled using a CR23X Datalogger (Campbell Scientific). There are two CR23X at each station, with each datalogger supporting two flow meters. Each station is powered by a pair of batteries charged by photovoltaic panels. A wireless cell data modem provides telemetry to each site. The flowmeters were installed and operated for SFWMD by Rapid Creek Research during 2006-2009. Desert Research Institute (DRI) was contracted by SFWMD to conduct a Quality Assurance/Quality Control (QA/QC) review and analysis of the data. The procedures followed for the QA/QC analysis are described here.

II. Data Flow

Data files retrieved from the loggers have a "table-based" format that includes header information that identifies each data field. Each logger saves at least two types of data files. The first file contains the raw data collected at the station, with the time interval varying from 1 minute to hourly. The second file contains metadata including specific site information, probe characteristics, serial numbers, and calibration information. The metadata file is updated hourly. Data files were provided for the period of record by Rapid Creek Research. Data files were updated by IP-based telemetry on a 15-minute interval and are saved as comma-delimited (.csv) file on the host computer at DRI. New data present in these data files are automatically ingested into a MySQL database on a roughly two-minute interval. Within the database, data reside in three different database tables: "Raw", "QA/QC", and "Finalized". Data first enter the database and are placed in the Raw Table; this data is never modified or altered. On a 30-minute basis, new data from the Raw Table are automatically copied into the QA/QC Table. Erroneous data in this table can be modified for quality control purposes and data quality ranks are assigned using a customized graphical user interface (GUI) based program (QAdjuster). All modifications to the data are logged with user, date time, the type of change (e.g. deletion, interpolation), and the mathematical parameters used to carry out the change. New data fields can also defined in the QA/QC Table based on mathematical formulas incorporating one or more existing data fields. This calculated variable feature permits the use of different formulas for different time periods. Once the erroneous data have been corrected and flagged with a QC ranking code, the user then marks each data point as finalized, triggering an automatic copying of those data points from the QA/QC Table into the Finalized Table. At DRI, a

Data Technician will be responsible for correcting erroneous data and applying QC ranking codes as described below. The Data Supervisor will be responsible for checking the accuracy of the data corrections and finalizing corrections.

III. Quality Control Practices

Data may be erroneous for many reasons, including electrical interference, sensor removal during site visits, instantaneous spikes or peaks, sensor drift, sensor fouling and data transmission errors. The purpose of quality control practices are to identify erroneous data, assess if a data correction should be applied, and finally to rank the accuracy of the continuous data based on field calibration checks.

Field QA of groundwater flowmeters (under separate contract with Rapid Creek Research) will include a visual verification that the suspension rods are properly installed, oriented vertically, and oriented with respect to north. If a groundwater flowmeter is changed, datalogger variables containing flowmeter serial numbers and calibration coefficients will be verified. Groundwater velocity data will be reviewed in conjunction with hydraulic head data to identify possible fouling such as by sediment accumulation, or for flowmeter malfunctions.

II.a. Identification and Correction of Erroneous Data

Data will be visually assessed for anomalies and outliers that diverge from field calibration checks and from current data trends from not only the sensor itself but with other sensors co-located in the same well, and other sensors at appropriate nearby sites.

The following rules govern the correction of erroneous data within the QA/QC database table:

1. Missing or erroneous data due to known causes (e.g. during site maintenance):
    a. Will be interpolated if:
        i. missing or erroneous data was less than three consecutive hours in duration, and;
        ii. the trend (slope) of data during the hour preceding the questionable data is within 10% of that measured during the first hour after the questionable data.
    b. Will be removed from the data set if the duration of questionable data is longer than three consecutive hours.

2. Correction of erroneous data due to sensor drift, fouling, or unknown origin:
    a. Will be conducted by interpolation if the erroneous data is considered to be a spike or anomaly defined as:
        i. one to three consecutive erroneous data points, and;
        ii. if the value of the spike/anomaly exceeds 3 times the criteria that result in a Poor quality ranking (see Section IIIb).
    b. Will be conducted by either a constant or variable corrections.
    c. If a malfunction occurs in up to two of the flowmeter's four thermistor pairs, flow direction and velocity will be calculated from the remaining thermistor pairs.

3. The heat pulse flowmeters have a pair of opposing thermistors on each of four poles (N-S, E-W, NE-SW, and SE-NW). Flowmeter velocity and direction will be calculated using 2 or 3 poles, if 2 or 1 poles, respectively, are determined to be malfunctioning. The direction will be calculated from the X- and Y-orientation of the 2 or 3 available correct directions (of N-S, E-W, NE-SW, and SE-NW poles). Velocity will be calculated from X- and Y-orientation of the 2 or 3 available correct directions (of N-S, E-W, NE-SW, and SE-NW poles).

Interpolation is the process where missing or erroneous data are corrected by linearly interpolating values based on known good points before and after the questionable data. The constant correction approach entails adding an unchanging modifier to all questionable data in a given time period. This approach would be used, for example, to correct data if a sensor during field calibration was misread. The variable correction approach uses a changing modifier to correct questionable data. This modifier normally starts at zero at the beginning of the time period and proportionally increases until it reaches its maximum value at the end of the time period. Variable corrections are typically used to correct for events that continue to aggregate through time, such as sensor drift and biofouling. If the start time of a variable correction cannot be specifically determined, the time of the last field calibration check will be used.

Data corrections discussed above are accomplished through a GUI-based interface in the QAdjuster program. This program also stores metadata associated with the correction to the database, including time of correction, user, correction type, reason for correction, and numeric coefficients used to perform the correction. A report detailing all corrections applied to the dataset can be subsequently generated on request.

IIb. Assignment of Quality Rating Codes.

The nature of the heat pulse groundwater flow measurement technique is such that accuracy cannot be determined by comparison against a standard or otherwise calibrated in the field. The velocity measurement procedure produces a vector magnitude that is converted to a velocity value based on laboratory calibration of the equipment. Quality rating may be evaluated based on the degree to which the characteristics of the thermal field generated in response to the heat pulse matches the ideal pattern obtained during calibration. Measurement accuracy is improved by temperature output that has characteristics that include: i) a stable baseline, ii) sufficient magnitude relative to detection limit, iii) clean temperature curves with relatively little noise, and iv) absence of direction reversal of the differential temperature trend suggestive of unimpeded flow through the probe, and v) number of poles for which data are available. Each data point will be assigned a quality code (Table C1) to rate the accuracy of the continuous reading relative to these characteristics. There are four possible ratings (poor, fair, good, and excellent) and are assigned a numeric code of 2 to 5, respectively, in the database.

Table C1. Accuracy ratings of continuous water-quality records.

Field Parameter	Quality Assurance Accuracy Ratings[1]			
	Excellent(5)	**Good(4)**	**Fair(3)**	**Poor(2)**
Groundwater Direction & Velocity	4 thermistor pairs w/stable baseline, magnitude > 20% of full scale	3 thermistor pairs w/ stable baseline or magnitude < 20% of full scale	2 thermistor pairs w/ stable baseline or magnitude < 10% of full scale	2 thermistor pairs w Unstable baseline or magnitude < 5% of full scale

[1] Numbers in parentheses refer to the numeric code assigned by QAdjuster. Internally, a code of 1 is used to denote suspect data for further evaluation or invalid data, and a code of 0 is assigned to data that has not yet undergone the QC process.

Prepared by: R.Susfalk, B.Fitzgerald and J.Brock (DRI)
Version 1.0
Revised: 1 March 2012

APPENDIX D. SUPPORTING DATA

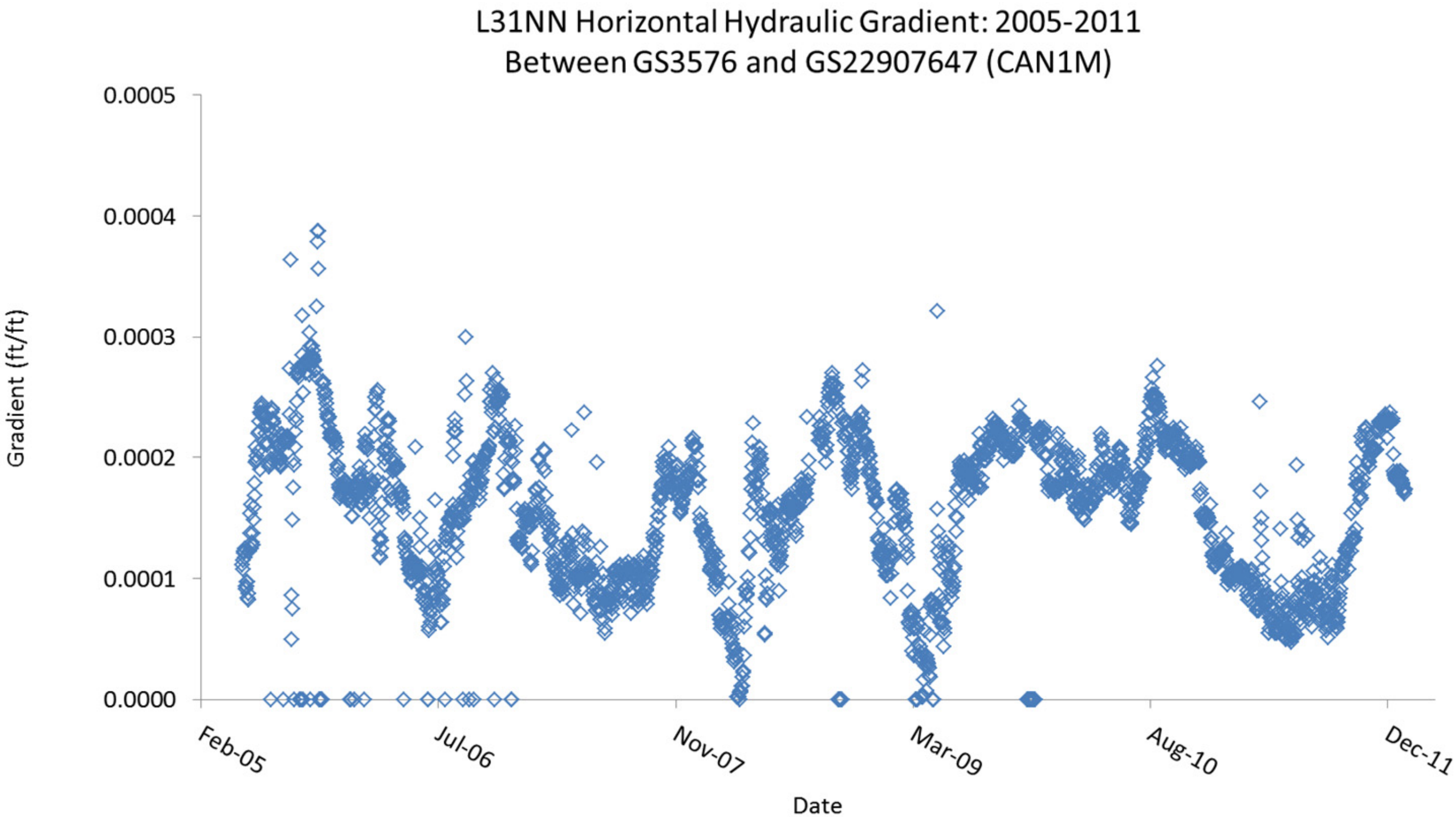

Figure D1. Horizontal hydraulic gradient for L31NN for 2005-2011.

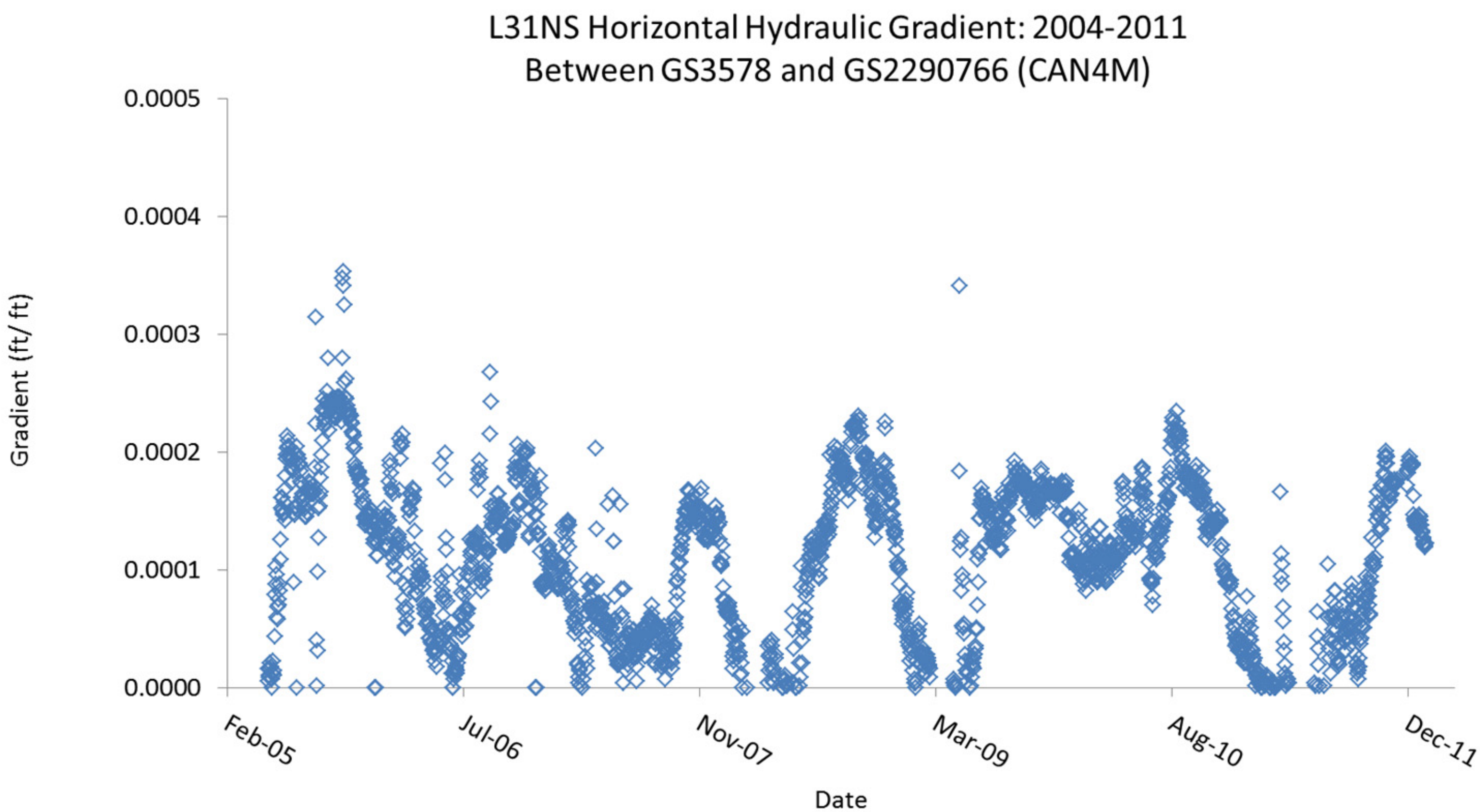

Figure D2. Horizontal hydraulic gradient for L31NS for 2005-2011.

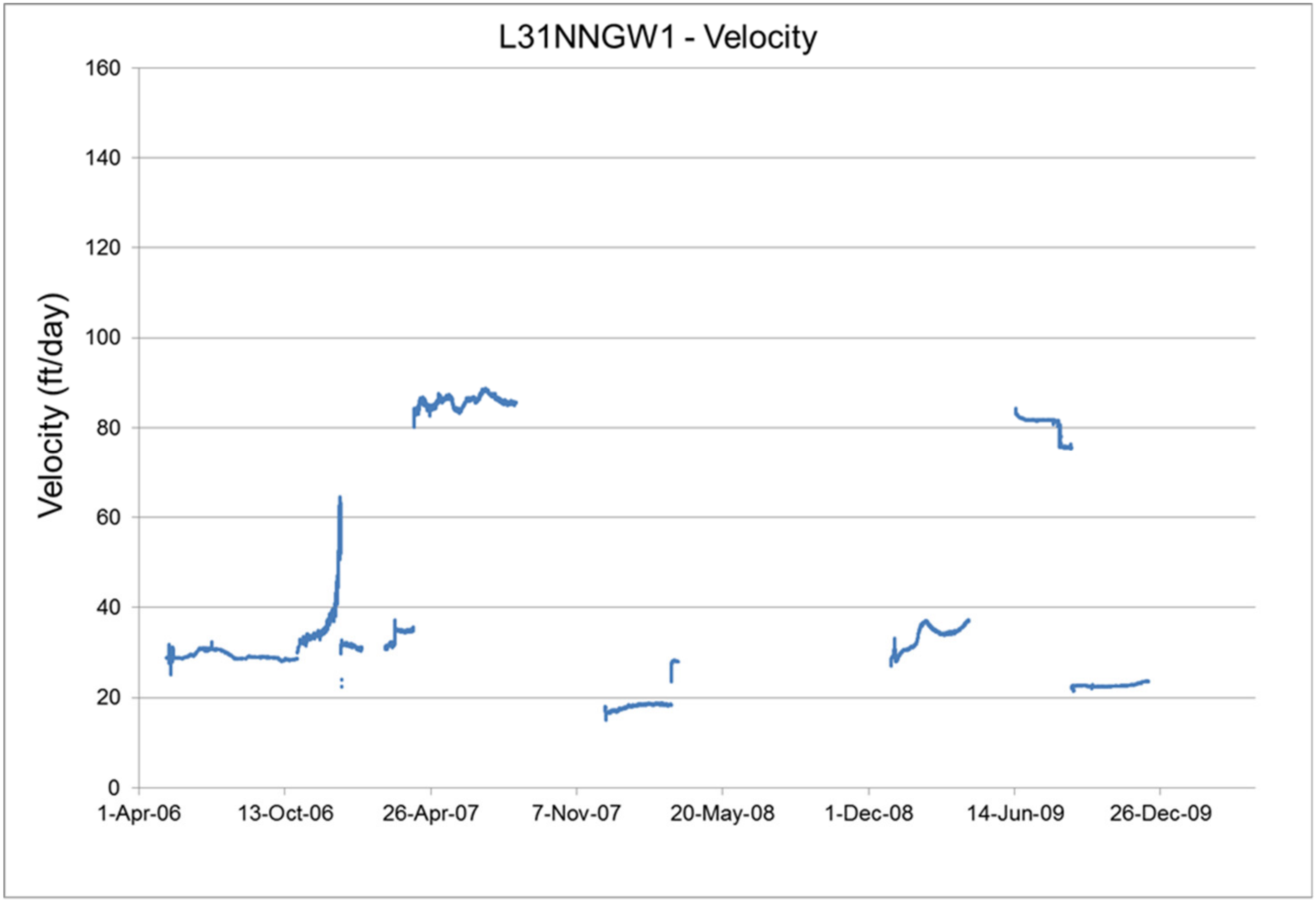

Figure D3. Velocity of L31NN GW1 during 2006-2009.

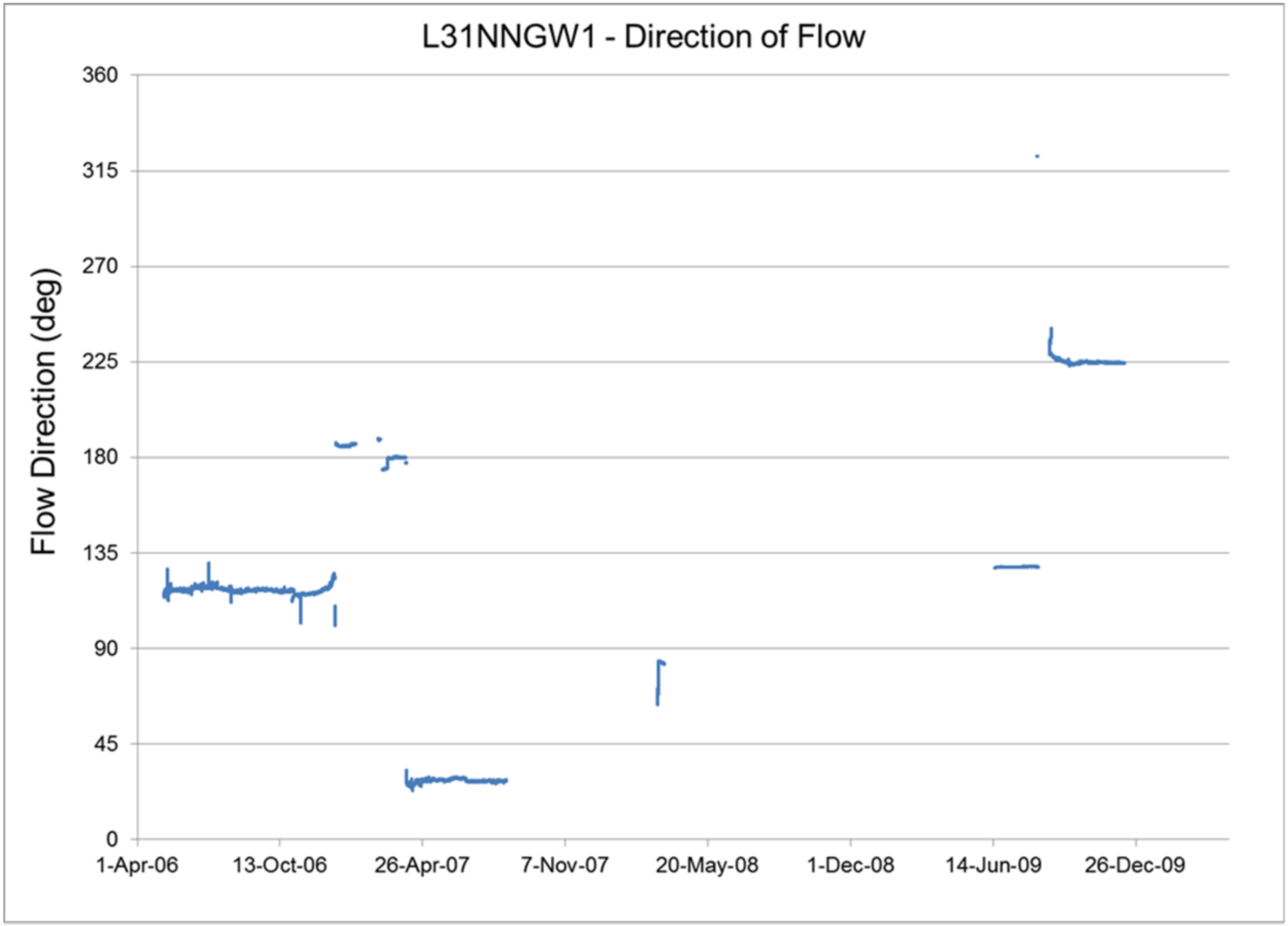

Figure D4. Direction of flow of L31NN GW1 during 2006-2009.

Figure D5. Velocity of L31NN GW2 during 2006-2009

Figure D6. Direction of flow of L31NN GW2 during 2006-2009.

Figure D7. Velocity of L31NN GW3 during 2006-2009

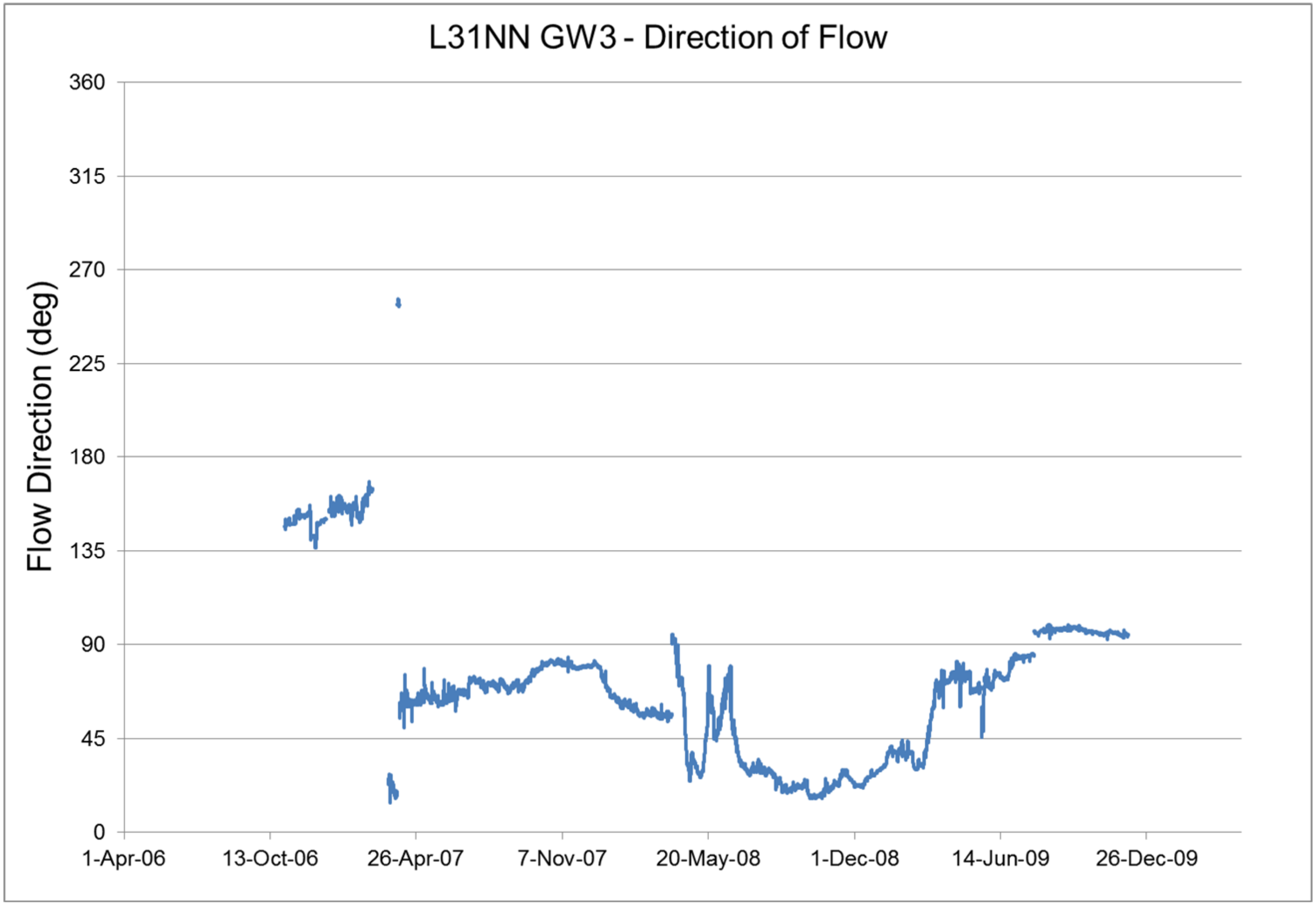

Figure D8. Direction of flow of L31NN GW3 during 2006-2009.

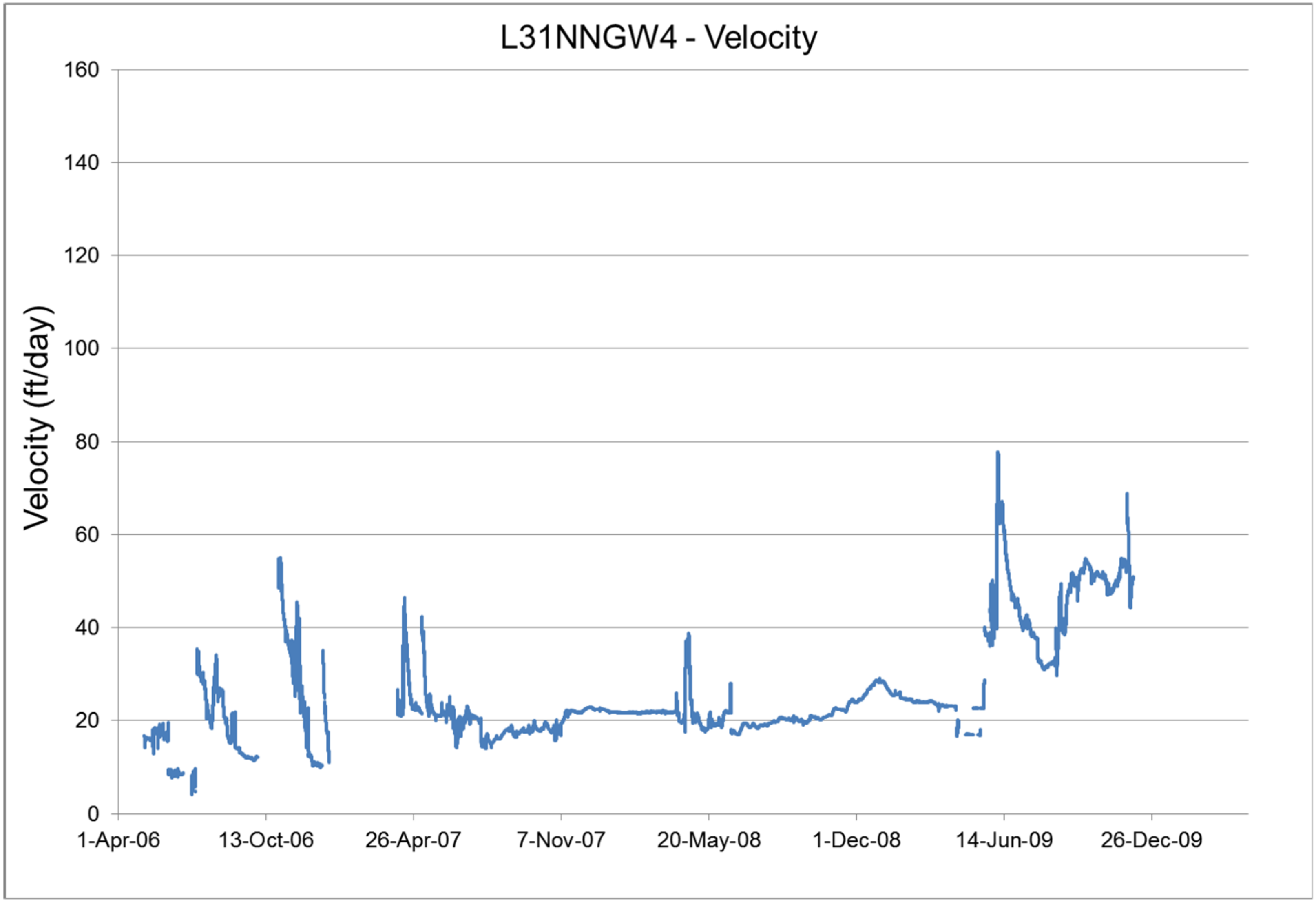

Figure D9. Velocity of L31NN GW4 during 2006-2009.

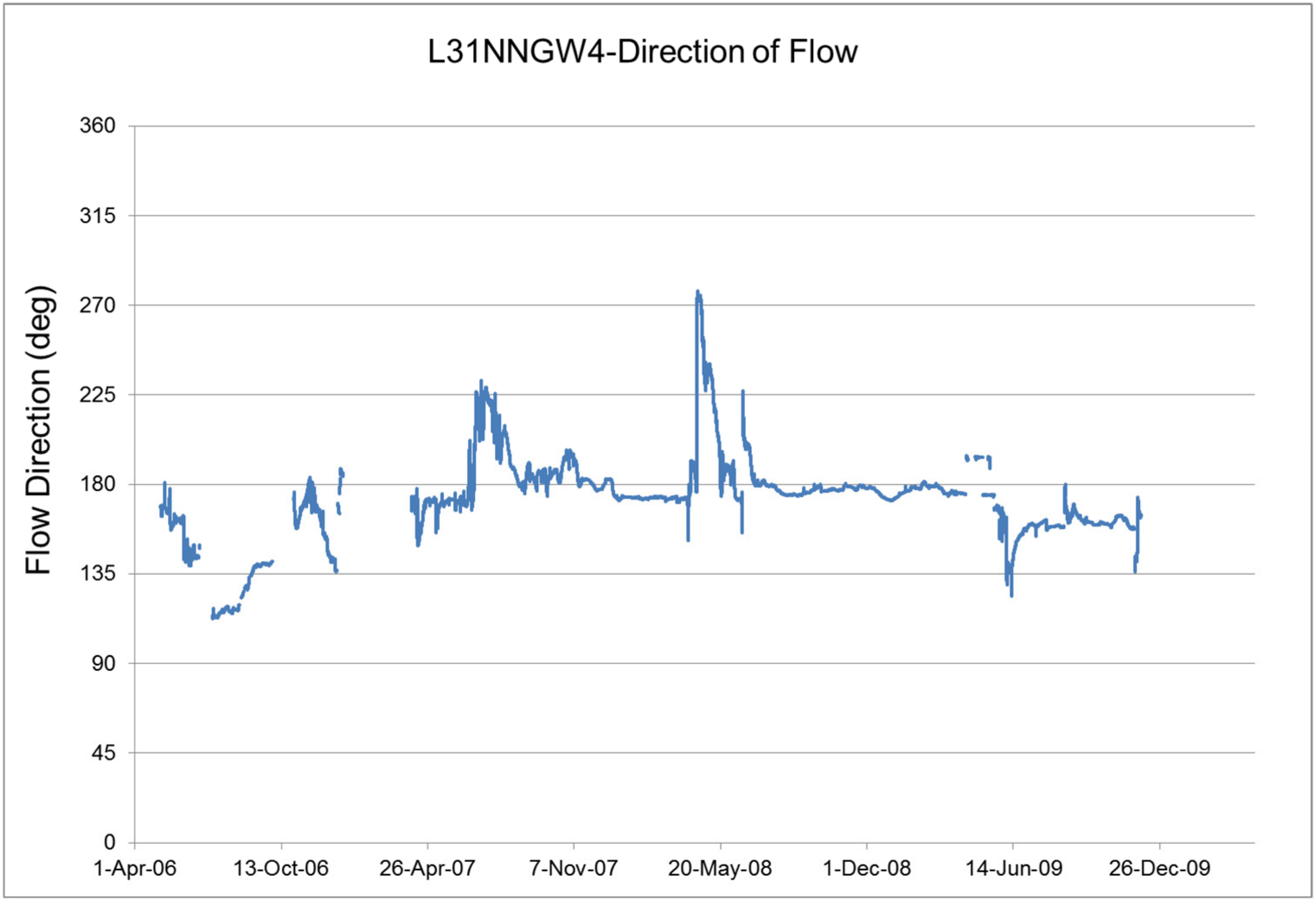

Figure D10. Direction of L31NN GW4 during 2006-2009

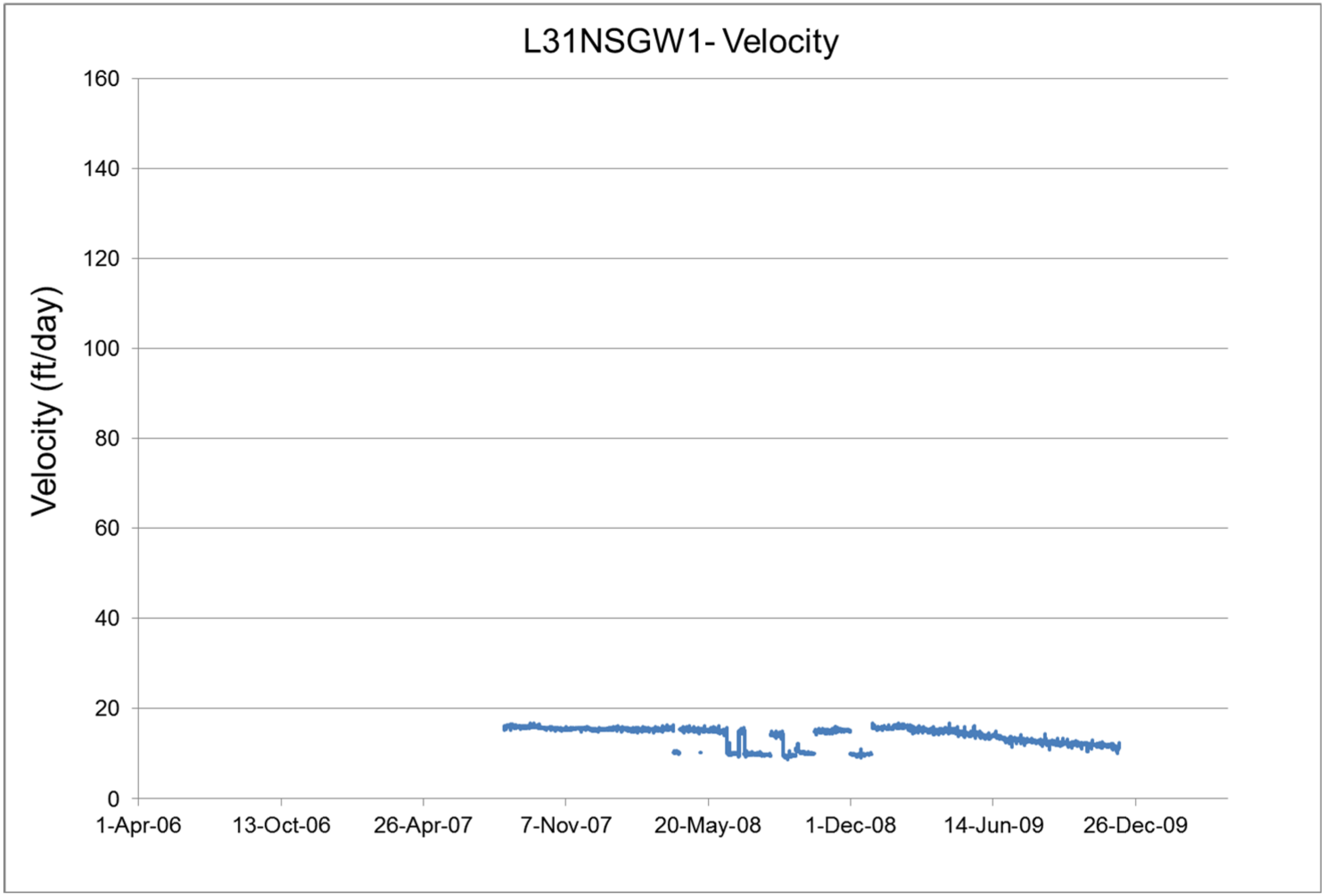

Figure D11. Velocity of L31NSGW1 during 2006-2009.

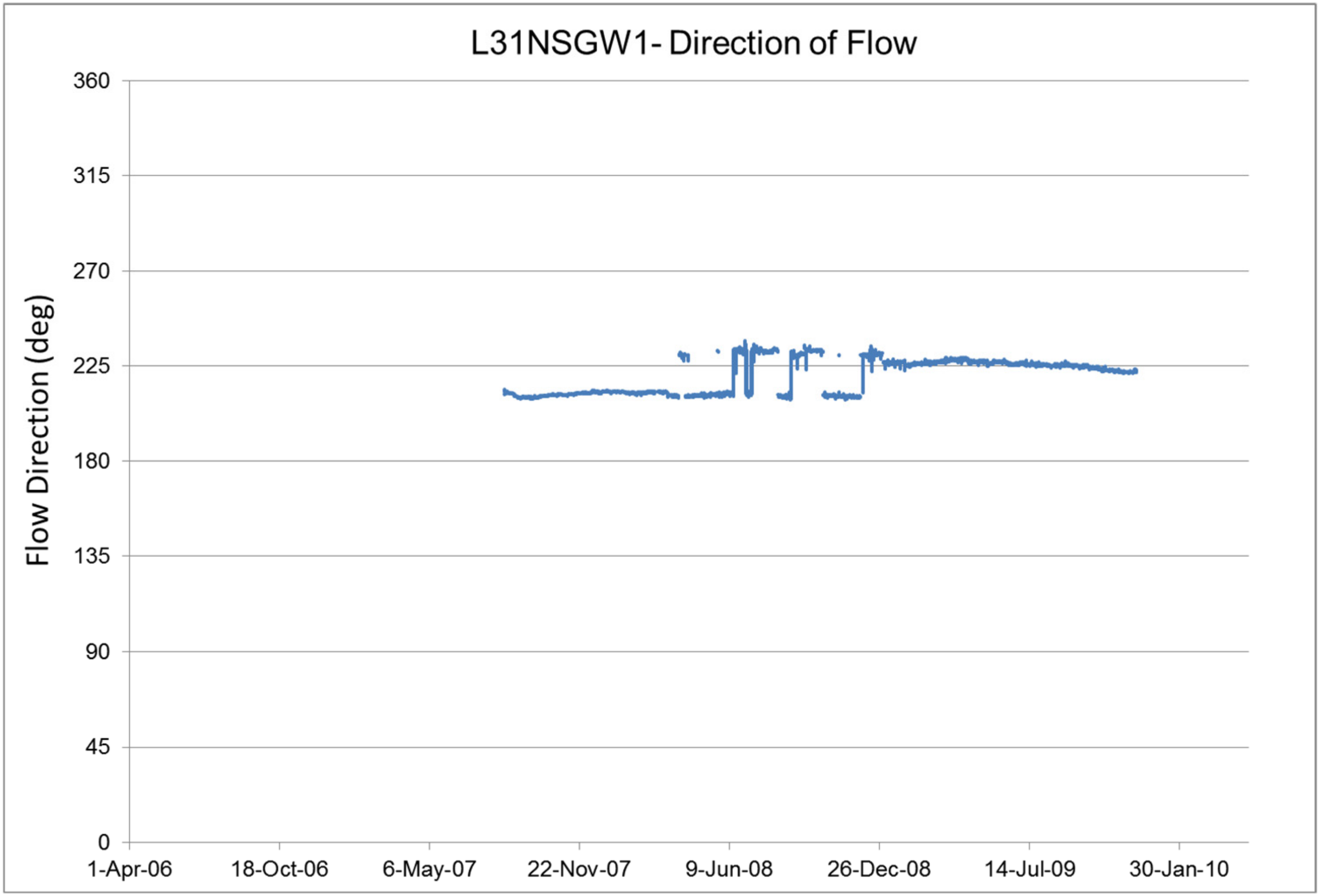

Figure D12. Direction of flow of L31NSGW1 during 2006-2009.

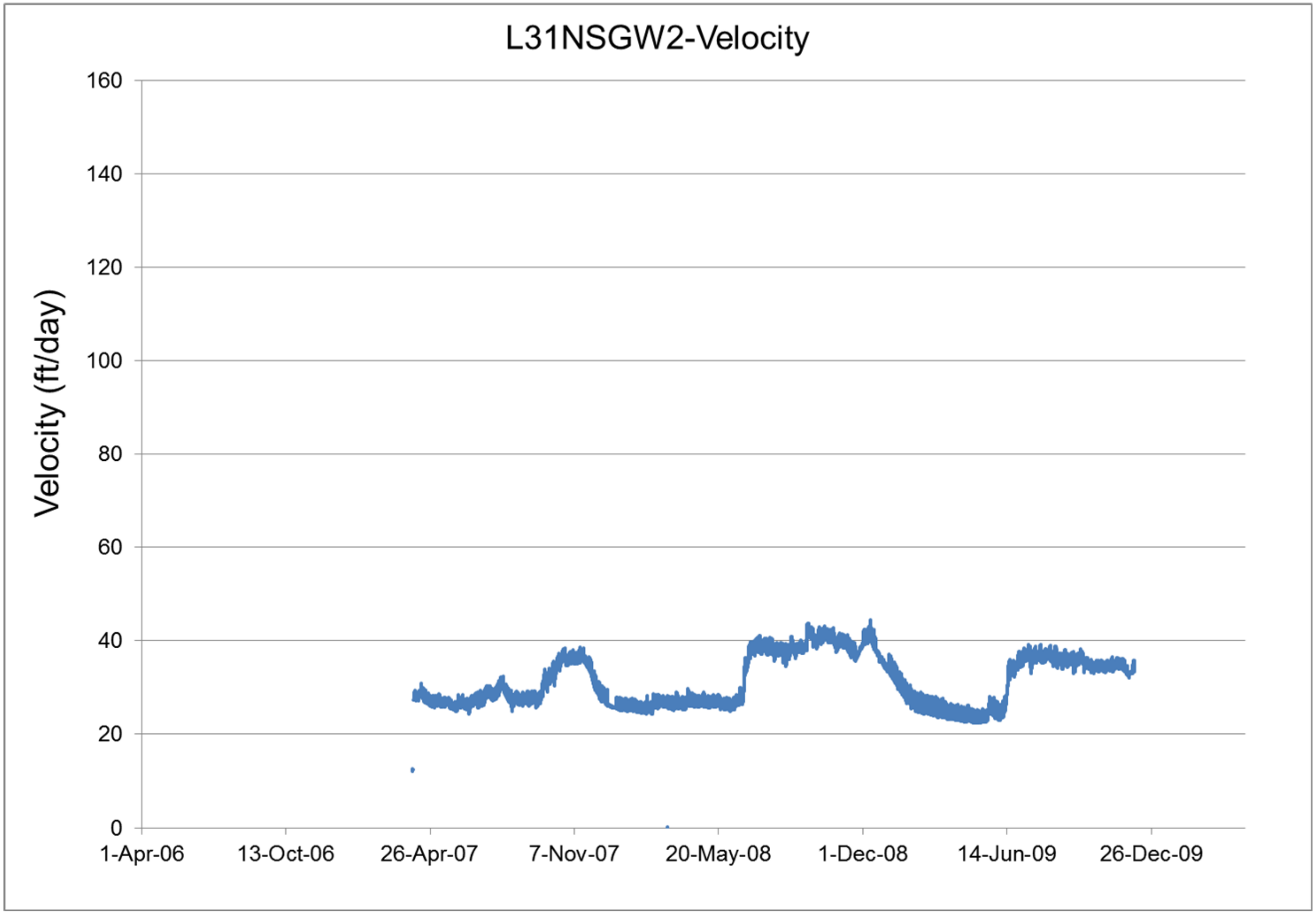

.

Figure D13. Velocity of L31NSGW2 during 2006-2009.

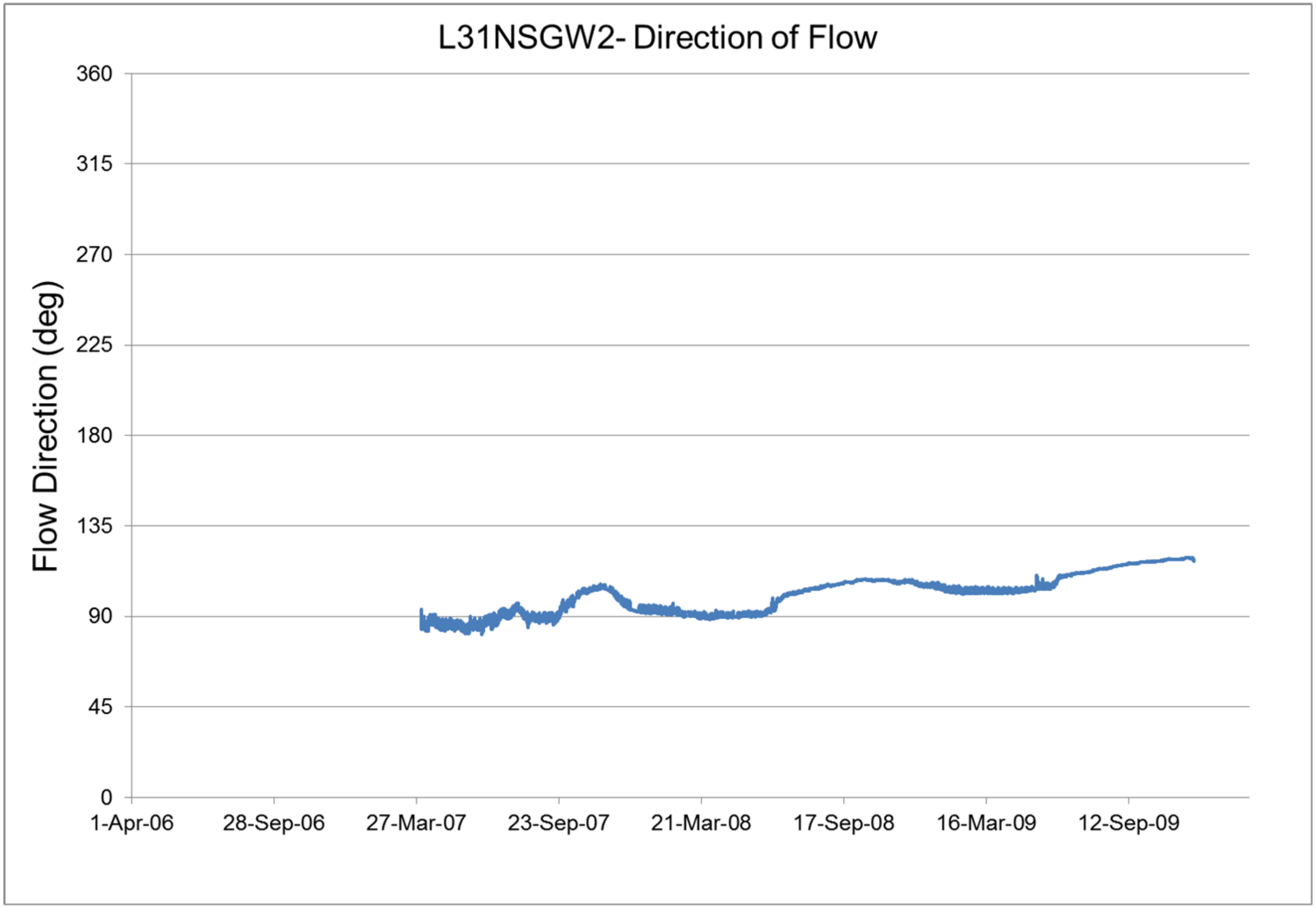

Figure D14. Direction of flow of L31NSGW2 during 2006-2009.

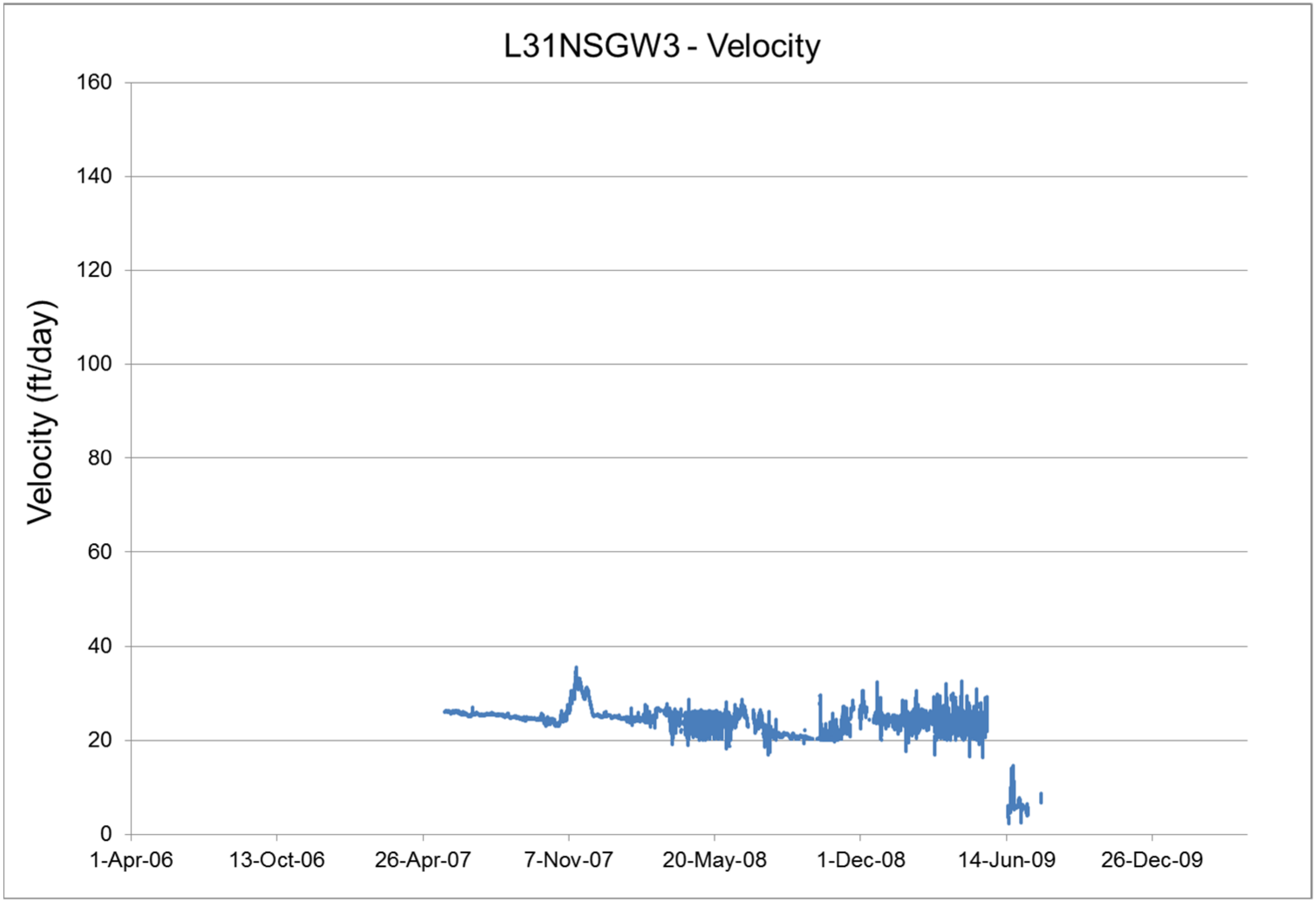

Figure D15. Velocity of L31NSGW3 during 2006-2009.

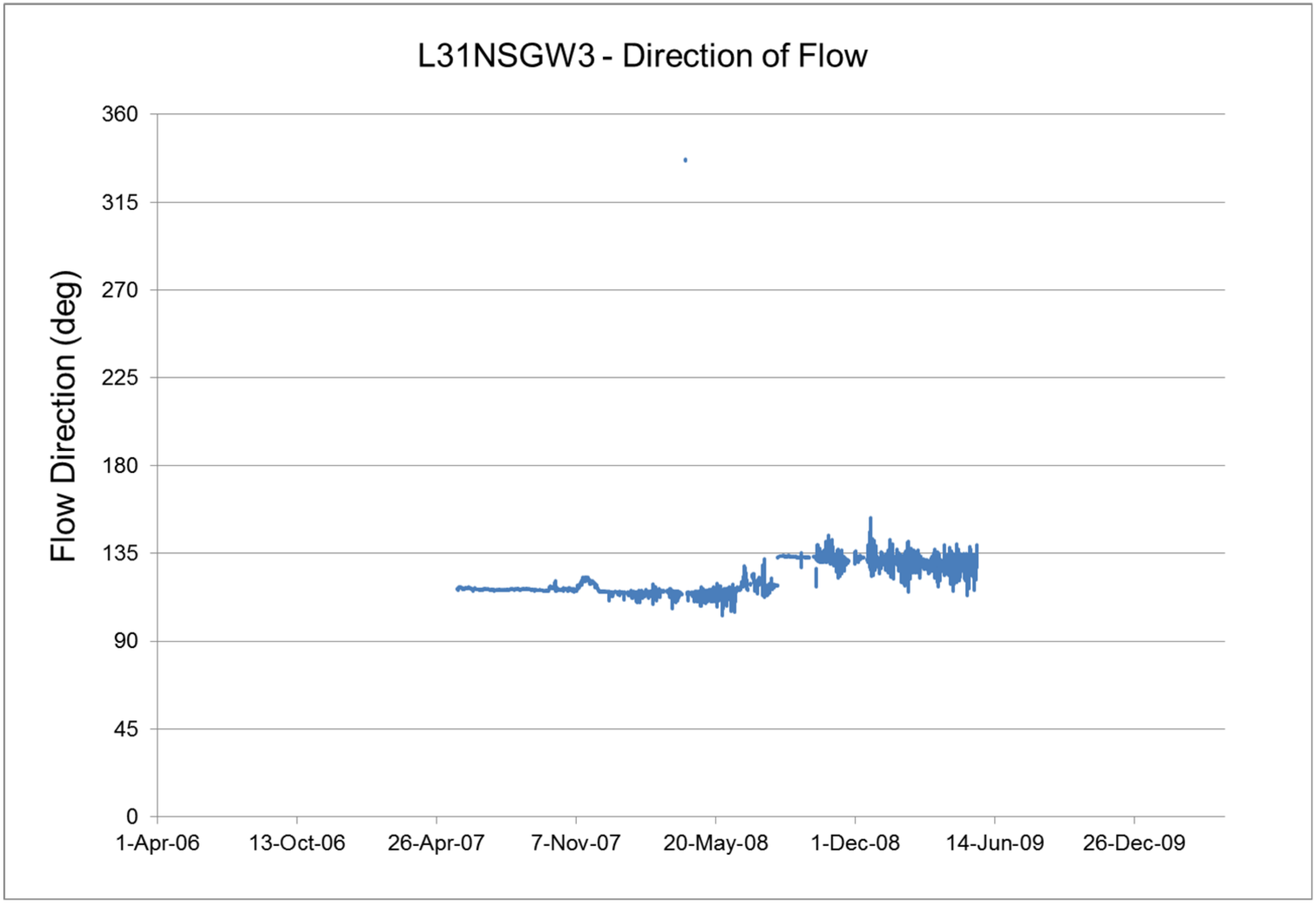

Figure D16. Direction of flow of L31NSGW3 during 2006-2009.

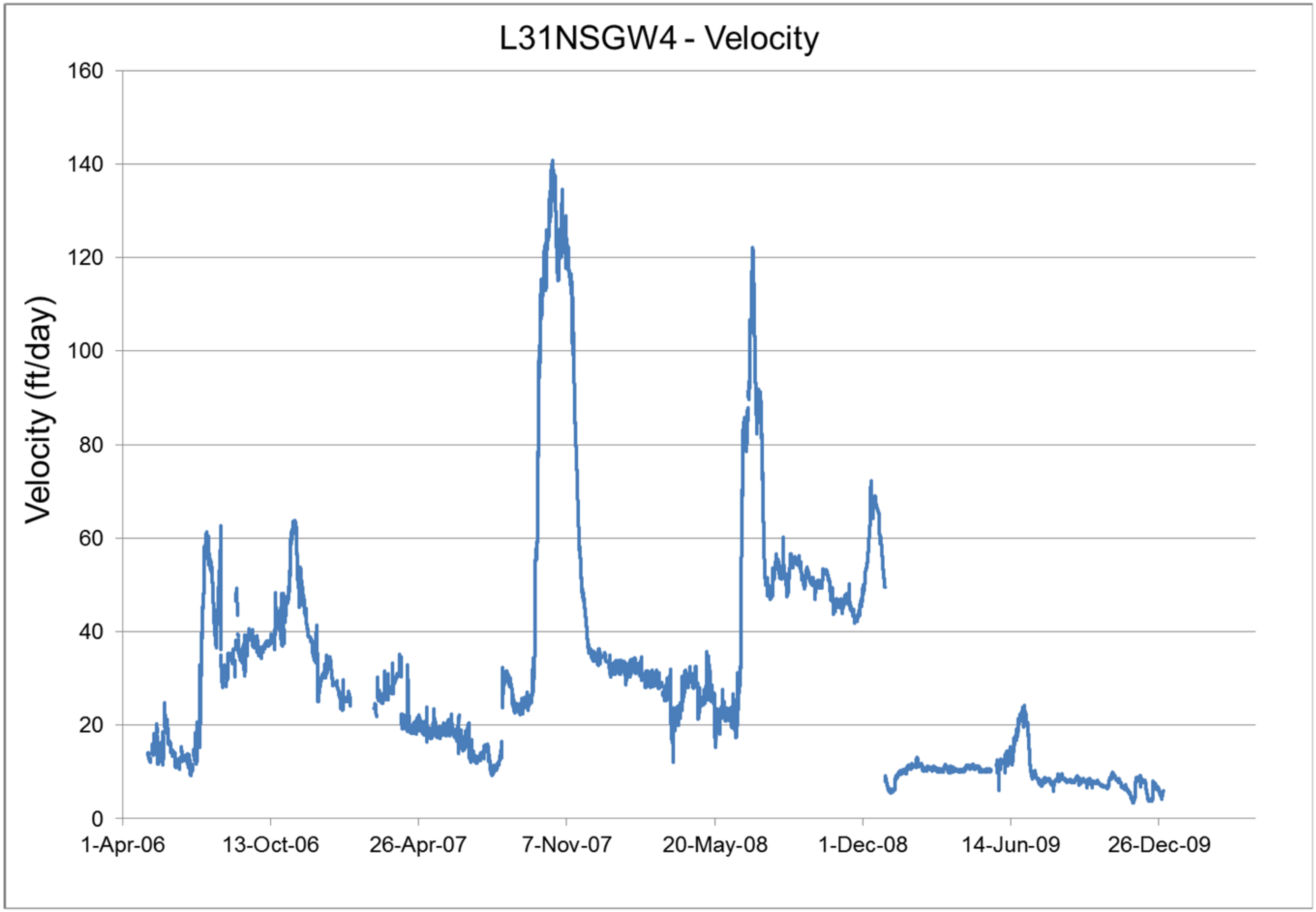

Figure D17. Velocity of L31NSGW4 during 2006-2009.

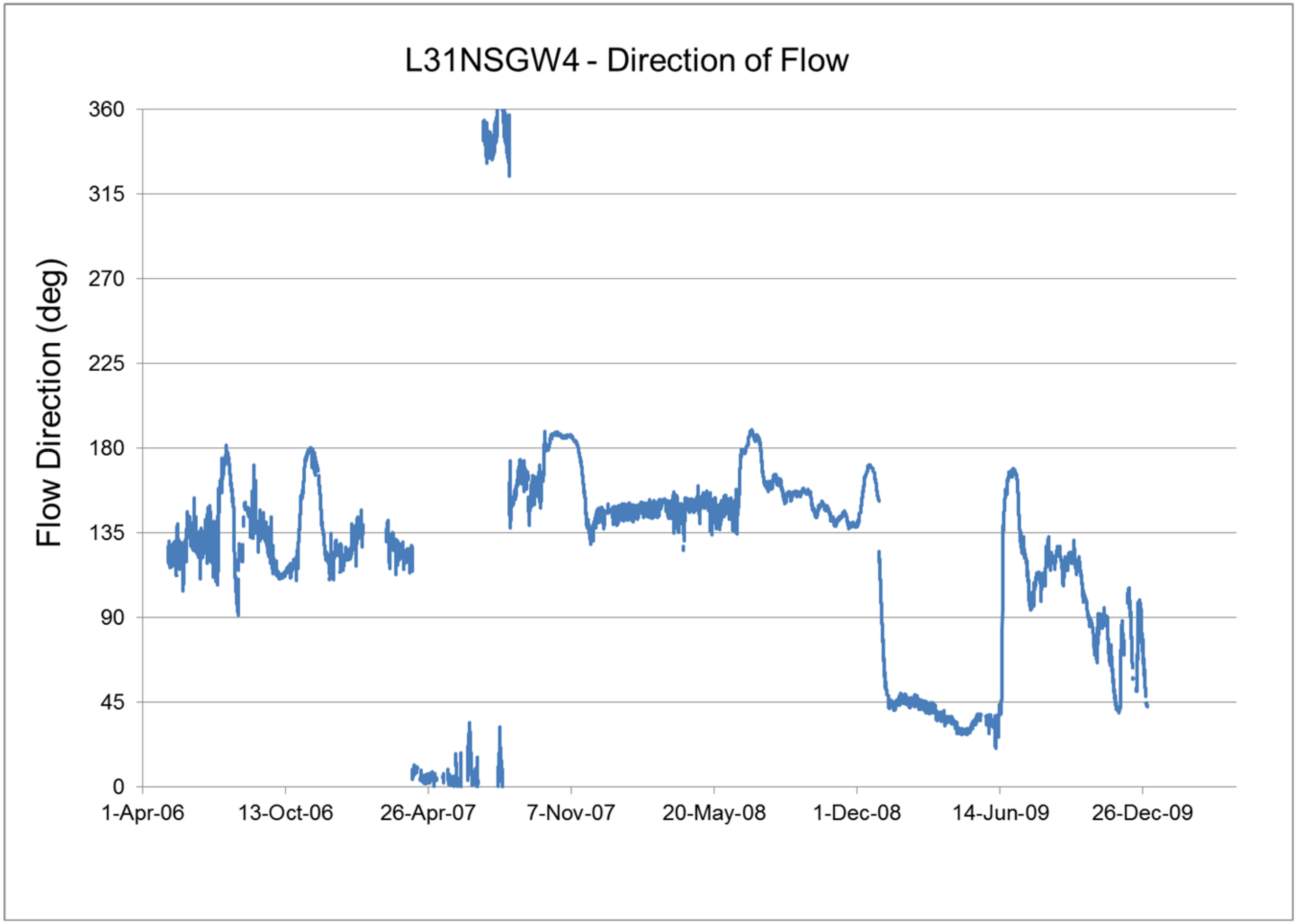

Figure D18. Direction of flow of L31NS GW4 during 2006-2009.

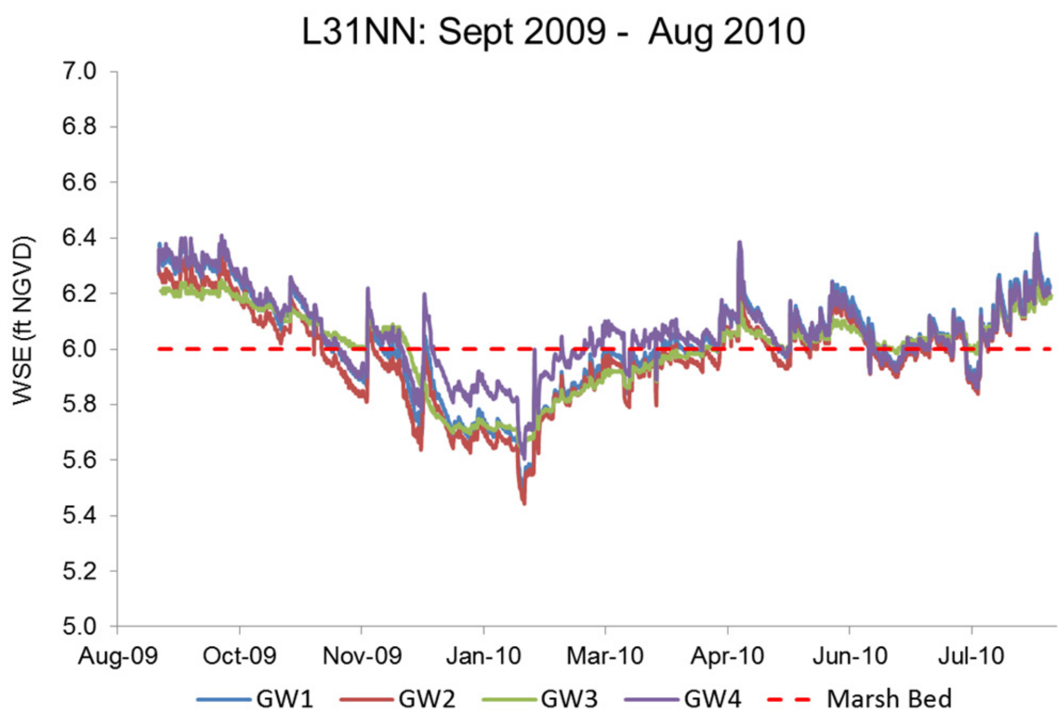

Figure D19. Water Surface Elevation (WSE) of L31NN wells Sept 2009-Aug 2010.

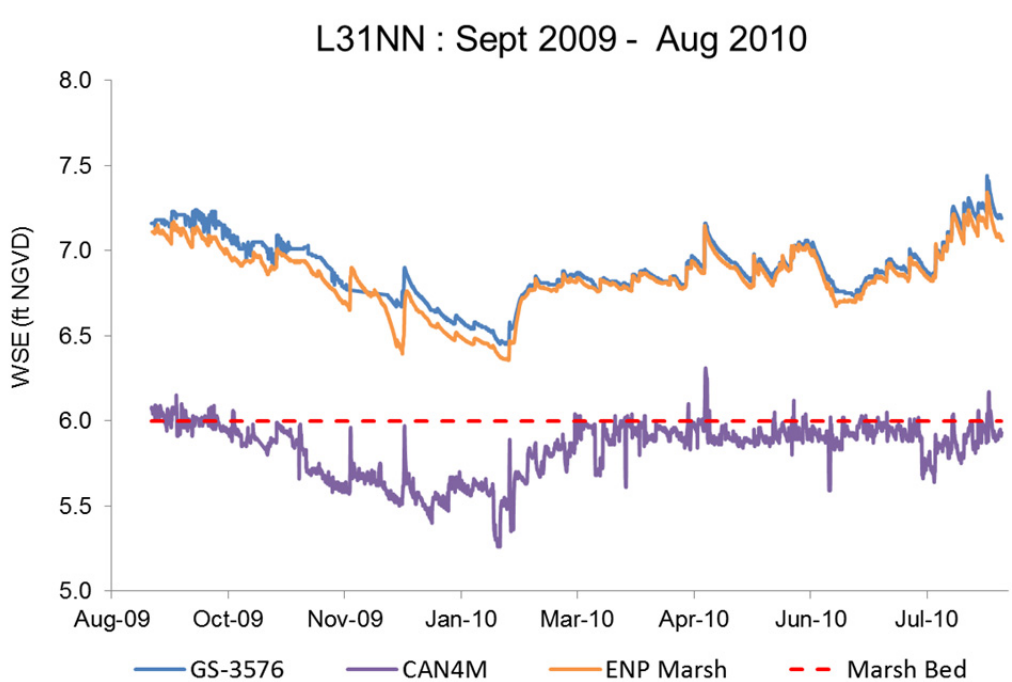

Figure D20. Water Surface Elevation (WSE) of L31NN vicinity Aug 2009-Aug 2010.

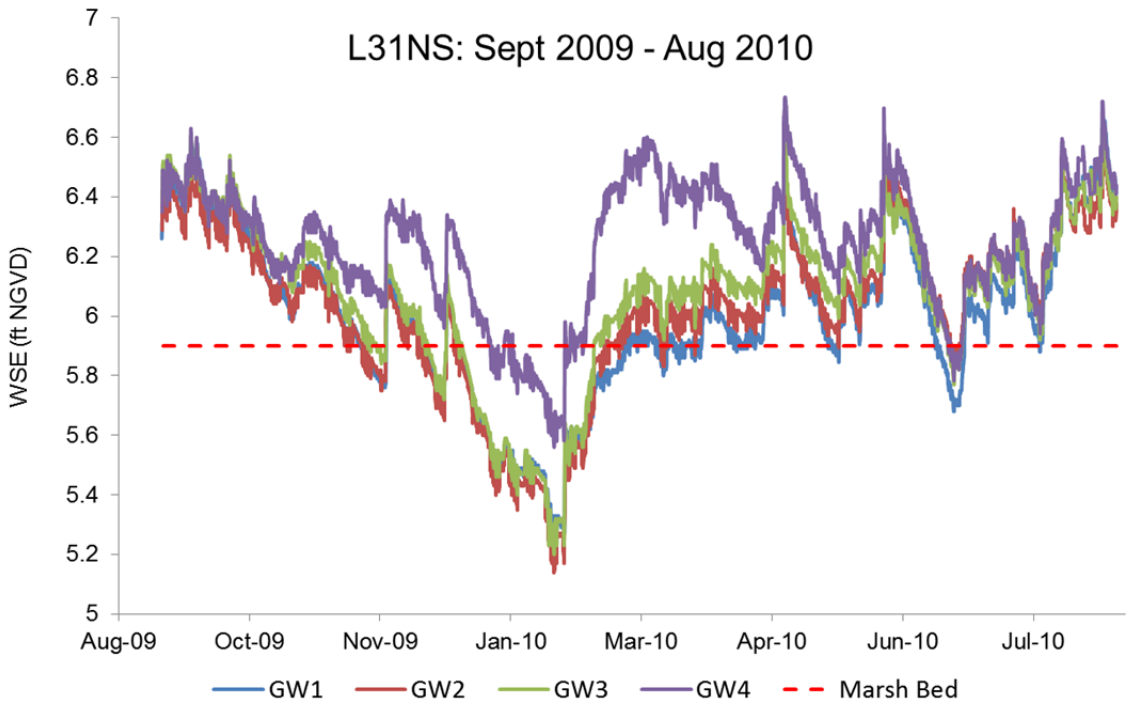

Figure D21. Water Surface Elevation (WSE) of L31NS wells Aug 2009-Aug 2010.

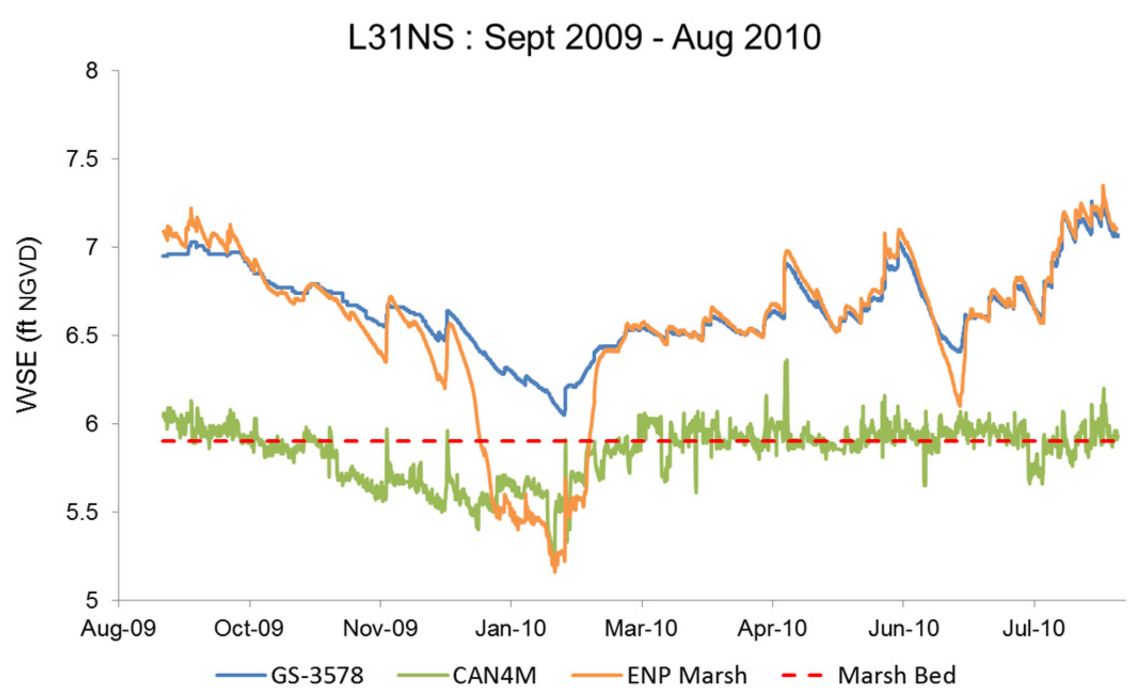

Figure D22. Water Surface Elevation (WSE) of L31NS vicintity Aug 2009-Aug 2010.

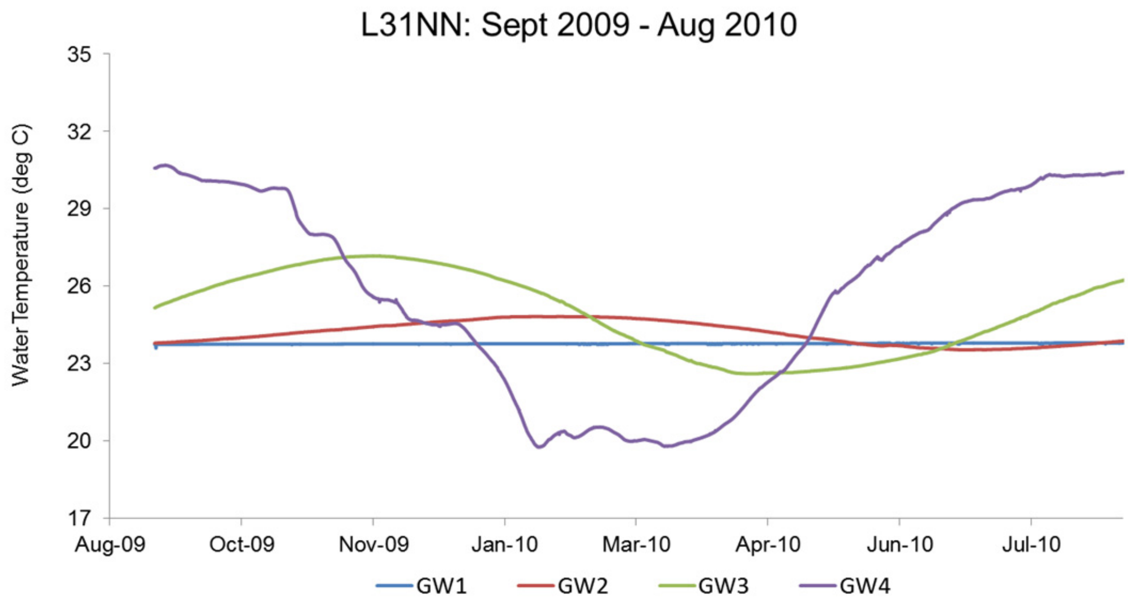

Figure D23. Water Temperature of L31NN Wells Sept 2009-Aug 2010

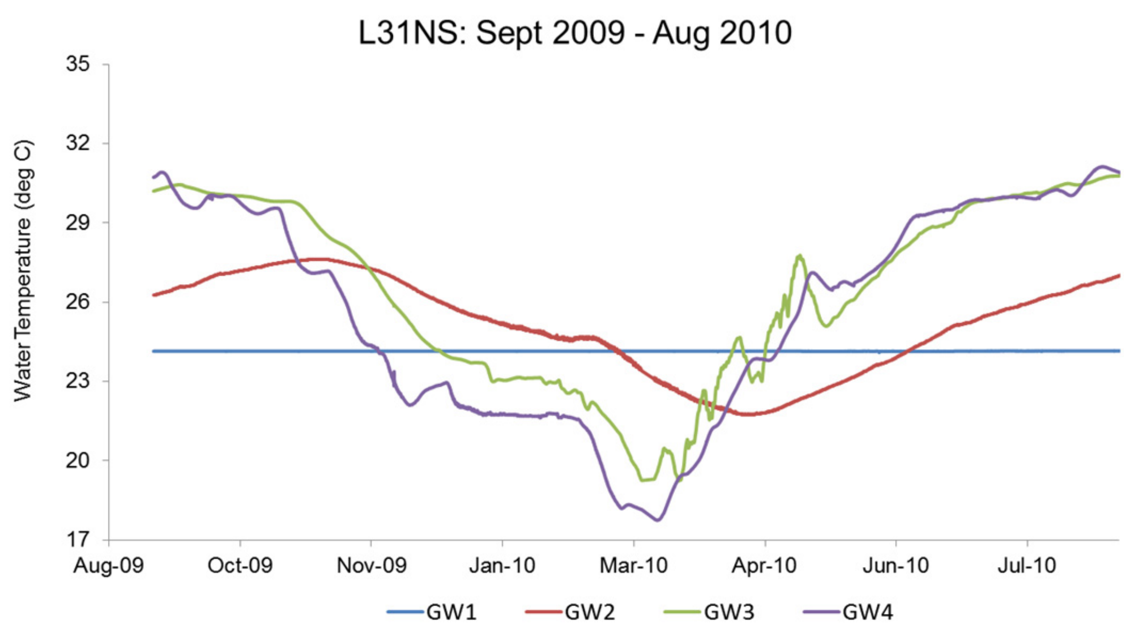

Figure D24. Water Temperature of L31NN Wells Sept 2009-Aug 2010

APPENDIX E. APPLICATION OF HORIZONTAL HEAT PULSE FLOWMETER TO LONG TERM MONITORING OF HYDROLOGICAL FLUX IN BISCAYNE AQUIFER, MIAMI-DADE, FLORIDA.

J.T. Brock and S. L. Krupa, Manuscript in Preparation